การยับยั้งการทำงานของเอนไซม์ฮีสโตนดีอะเซทิเลสเสริมการแปรสภาพไปเป็นเซลล์สร้างกระดูก
ของเซลล์เอ็นยึดปริทันต์ของมนุษย์

นายฮุน กอง นัท นาม

วิทยานิพนธ์นี้เป็นส่วนหนึ่งของการศึกษาตามหลักสูตรปริญญาวิทยาศาสตรดุษฎีบัณฑิต
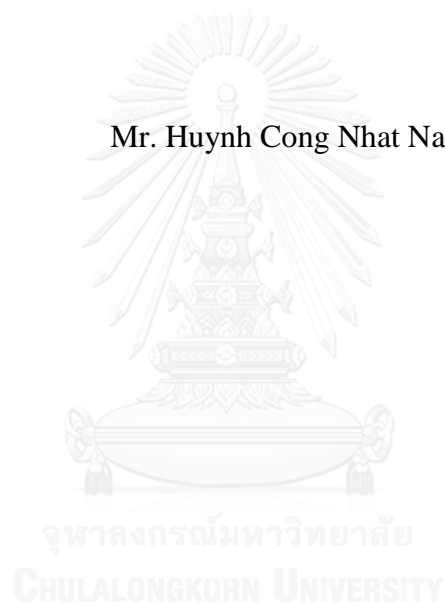สาขาวิชาชีววิทยาช่องปาก
คณะทันตแพทยศาสตร์ จุฬาลงกรณ์มหาวิทยาลัย
ปีการศึกษา 2558
ลิขสิทธิ์ของจุฬาลงกรณ์มหาวิทยาลัย

INHIBITION OF HISTONE DEACETYLASES ENHANCES OSTEOGENIC

DIFFERENTIATION OF HUMAN PERIODONTAL LIGAMENT CELLS

Mr. Huynh Cong Nhat Nam

A Dissertation Submitted in Partial Fulfillment of the Requirements
for the Degree of Doctor of Philosophy Program in Oral Biology
Faculty of Dentistry
Chulalongkorn University
Academic Year 2015
Copyright of Chulalongkorn University

Thesis Title	INHIBITION OF HISTONE DEACETYLASES ENHANCES OSTEOGENICDIFFERENTIATION OF HUMAN PERIODONTAL LIGAMENT CELLS
By	Mr. Huynh Cong Nhat Nam
Field of Study	Oral Biology
Thesis Advisor	Associate Professor Dr. Ruchanee Ampornaramveth
Thesis Co-Advisor	Professor Dr. Prasit Pavasant

Accepted by the Faculty of Dentistry, Chulalongkorn University in Partial Fulfillment of the Requirements for the Doctoral Degree

....Dean of the Faculty of Dentistry
(Assistant Professor Dr. Suchit Poolthong)

THESIS COMMITTEE

....Chairman
(Assistant Professor Dr. Jeerus Sucharitakul)

....Thesis Advisor
(Associate Professor Dr. Ruchanee Ampornaramveth)

....Thesis Co-Advisor
(Professor Dr. Prasit Pavasant)

....Examiner
(Associate Professor Dr. Oranart Matangkasombut)

....Examiner
(Assistant Professor Dr. Thanaphum Osathanoon)

....External Examiner
(Assistant Professor Dr. Weerachai Singhatanadgit)

ฮุน กอง นัท นาม : การยับยั้งการทำงานของเอนไซม์ฮีสโตนดีอะเซทิเลสเสริมการแปรสภาพไปเป็นเซลล์สร้างกระดูกของเซลล์ เอ็นยึดปริทันต์ของมนุษย์ (INHIBITION OF HISTONE DEACETYLASES ENHANCES OSTEOGENICDIFFERENTIATION OF HUMAN PERIODONTAL LIGAMENT CELLS) อ.ที่ปรึกษาวิทยานิพนธ์หลัก: รัชนี อัมพรอร่ามเวทย์, อ.ที่ปรึกษาวิทยานิพนธ์ ร่วม: ประสิทธิ์ ภวสันต์, 100 หน้า.

วัตถุประสงค์: เมื่อถูกกระตุ้นอย่างเหมาะสมเซลล์เอ็นยึดปริทันต์จะสามารถเจริญและพัฒนาไปเป็นเซลล์สร้างกระดูกได้ ดังนั้น เซลล์เอ็นยึดปริทันต์จึงเป็นหนึ่งในตัวเลือกที่ดีที่จะนำมาใช้ปลูกกระดูกทดแทนโดยใช้เซลล์จากเนื้อเยื่อของผู้ป่วยเอง งานวิจัยนี้มีวัตถุประสงค์ เพื่อศึกษาบทบาทของเอนไซม์ฮีสโตนดีอะเซทิเลสต่อการเจริญและพัฒนาไปเป็นเซลล์สร้างกระดูกของเซลล์เอ็นยึดปริทันต์มนุษย์ และผลของ สารยับยั้งเอนไซม์ฮีสโตนดีอะเซทิเลสในการเสริมประสิทธิภาพของการนำเซลล์เอ็นยึดปริทันต์มนุษย์มาใช้ในการปลูกกระดูกทดแทน

วิธีการ: การทำงานของเอนไซม์ฮีสโตนดีอะเซทิเลสถูกยับยั้งในเซลล์เอ็นยึดปริทันต์มนุษย์ด้วยไตรโคสแตตินเอ (ทีเอสเอ) ความ มีชีวิตของเซลล์ การแสดงออกของยีน การทำงานของเอนไซม์อัลคาไลน์ฟอสฟาเตสและการสะสมแร่ธาตุของกระดูกถูกวัดเพื่อประเมิน ความสามารถในการกลายสภาพเป็นเซลล์สร้างกระดูก ปริมาณโปรตีน RUNX2 ระดับการอะเซทิเลชันของฮีสโตนโปรตีน และปริมาณการ แสดงออกของเอนไซม์ฮีสโตนดีอะเซทิเลสถูกวัดด้วยเทคนิคเวสเทิร์นบลอท การสร้างกระดูกโดยใช้การเพาะเลี้ยงในห้องปฏิบัติการแบบสาม มิติและโมเดลการหายของแผลในกะโหลกศีรษะของหนูทดลองโดยใช้วัสดุโครงร่างโคโพลีเมอร์ (PCL/PEG) การวิเคราะห์ด้วยเทคนิคฮีสโตมอร์ โฟเมทริก การวิเคราะห์ภาพถ่ายไมโครซีที ถูกนำมาใช้เพื่อประเมินผลของทีเอสเอในการกระตุ้นการสร้างกระดูกในสัตว์ทดลอง ปฏิกิริยาทาง ภูมิคุ้มกันในหนูต่อเซลล์เอ็นยึดปริทันต์แปลกปลอมถูกวัดโดยเทคนิคอิมมูโนฮีสโตเคมิสทรี และ ELISA

ผลการทดลอง: ระหว่างการเจริญพัฒนาไปเป็นเซลล์สร้างกระดูกทีเอสเอสามารถกระตุ้นการแสดงออกของยีนที่เกี่ยวข้องกับการ สร้างกระดูก กระตุ้นการทำงานของเอนไซม์อัลคาไลน์ฟอสฟาเตสและการสะสมแร่ธาตุของกระดูกในเซลล์เอ็นยึดปริทันต์มนุษย์ได้ เซลล์เอ็นยึด ปริทันต์มนุษย์สามารถสร้างเอนไซม์ฮีสโตนดีอะเซทิเลสได้ทั้งคลาสที่หนึ่ง (HDAC 1, 2,3) และ คลาสที่สอง (HDAC 4, 6) ระหว่างการเจริญ พัฒนาไปเป็นเซลล์สร้างกระดูกการแสดงออกของเอนไซม์ฮีสโตนดีอะเซทิเลส 3 นั้นค่อยๆ ลดลงอย่างต่อเนื่อง การลดลงนี้เห็นชัดขึ้นเมื่อ มีสาร ยับยั้งการทำงานของเอนไซม์ฮีสโตนดีอะเซทิเลส ระดับการอะเซทิเลชันของฮีสโตน เอช 3 นั้นจะเพิ่มขึ้นในระหว่างการเจริญพัฒนาไปเป็น เซลล์สร้างกระดูก ทีเอสเอสามารถกระตุ้นให้เกิดการอะเซทิเลชั่นของฮีสโตน เอช 3 ที่เพิ่มขึ้นอย่างมาก และเพิ่มระดับการแสดงออกของโปรตีน RUNX2 ทีเอสเอสามารถส่งเสริมการสะสมแร่ธาตุของกระดูกโดยเซลล์เอ็นยึดปริทันต์มนุษย์ในการเพาะเลี้ยงแบบสามมิติในห้องปฏิบัติการ ความสามารถในการซ่อมแซมแผลในกะโหลกศีรษะของหนูด้วยเซลล์เอ็นยึดปริทันต์มนุษย์นั้นเพิ่มขึ้นอย่างมีนัยสำคัญด้วยทีเอสเอ การวิเคราะห์ ปริมาณกระดูกด้วยไมโครซีทีแสดงให้เห็นถึงปริมาณมวลกระดูก (BV/TV) เพิ่มขึ้นอย่างมีนัยสำคัญในกลุ่มที่มีการใช้ทีเอสเอทั้งที่ 4 และ 8 สัปดาห์ การย้อมด้วยเทคนิคอิมมูโนฮีสโตเคมิสทรีแสดงให้เห็นว่ามีเซลล์มนุษย์ถูกรวมอยู่ในกระดูกที่ถูกสร้างขึ้นใหม่บริเวณกะโหลกศีรษะหนู การตรวจซีรัมหนูด้วย ELISA แสดงให้เห็นว่าไม่มีปฏิกิริยาต่อต้านเซลล์มนุษย์อย่างมีนัยสำคัญ

สรุป: การศึกษานี้แสดงให้เห็นถึงรายละเอียดเพิ่มเติมถึงบทบาทการทำงานของเอนไซม์ฮีสโตนดีอะเซทิเลสในกระบวนการ พัฒนาไปเป็นเซลล์สร้างกระดูกของเซลล์เอ็นยึดปริทันต์มนุษย์ ไตรโคสแตตินเอสามารถกระตุ้นความสามารถในการสร้างกระดูกโดยเซลล์เอ็น ยึดปริทันต์มนุษย์ทั้งในห้องปฏิบัติการและในสัตว์ทดลอง ทำให้การนำเซลล์เอ็นยึดปริทันต์มนุษย์มาใช้ในการสร้างกระดูกทดแทนเป็นไปได้มาก ยิ่งขึ้น

สาขาวิชา ชีววิทยาช่องปาก	ลายมือชื่อนิสิต _____
ปีการศึกษา 2558	ลายมือชื่อ อ.ที่ปรึกษาหลัก _____
	ลายมือชื่อ อ.ที่ปรึกษาร่วม _____

5676054432 : MAJOR ORAL BIOLOGY

KEYWORDS: HDAC INHIBITOR / HISTONE DEACETYLASE / OSTEOGENIC DIFFERENTIATION / PERIODONTAL LIGAMENT CELL / TRICHOSTATIN A / BONE REGENERATION / TISSUE ENGINEERING

> HUYNH CONG NHAT NAM: INHIBITION OF HISTONE DEACETYLASES ENHANCES OSTEOGENICDIFFERENTIATION OF HUMAN PERIODONTAL LIGAMENT CELLS. ADVISOR: ASSOC. PROF. DR. RUCHANEE AMPORNARAMVETH, CO-ADVISOR: PROF. DR. PRASIT PAVASANT, 100 pp.

Objectives: When appropriately triggered, periodontal ligament (PDL) cells can differentiate into mineralized tissue forming cells, thus make it a good candidate for autologous bone graft. This study aimed to investigate the role of histone deacetylases (HDACs) in osteogenic differentiation of human PDL cells (hPDLs). The effect of HDAC inhibitor on an enhancement of bone regeneration by hPDL cells was also examined.

Methods: Activity of HDACs was blocked in primary hPDLs using the inhibitor trichostatin A (TSA). Cell viability, gene expression, ALP activity and mineral deposition assays were used to assess osteoblast phenotypes. RUNX2, histone acetylation and HDACs expression were also observed by western blot analysis. In vitro 3D culture and mouse calvarial defect model were performed using co-polymer scaffold (PCL/PEG). Histomorphometric analysis, micro-CT scan were used to evaluate the *in vivo* effect of TSA on bone regeneration. The immunogenic activity of mice against allogenic hPDLs was verified by immunohistochemistry staining and ELISA.

Results: During the osteogenic differentiation with TSA, osteoblast-related genes expression, ALP activity and bone nodule formation were accelerated. hPDLs highly expressed HDACs of class I (HDAC 1, 2, 3) and class II (HDAC 4, 6). During osteogenic differentiation, HDAC 3 expression gradually decreased. This effect was apparent in the presence of the inhibitor. The level of acetylated histone H3 increased during osteogenic differentiation while treatment with TSA induced histone H3 hyperacetylation and RUNX2 protein expression. TSA enhanced mineral deposition by hPDLs in in-vitro 3D culture model. In vivo bone regeneration potential of hPDLs in mouse calvarial defect model was significantly enhanced by TSA treatment. Micro-CT analysis demonstrated the significant increase of BV/TV in inhibitor treated groups at 4 and 8 weeks. Immunohistochemistry staining demonstrated human cells incorporate into newly form osseous tissues of mice calvarias. While ELISA of mice serum indicated no significant immune reactivity against xenogenic human cells.

In conclusion: This study provided further insight into the roles of HDACs function in osteogenic differentiation of hPDLs. TSA enhanced both *in vitro* and *in vivo* bone regeneration potential of hPDLs making its more applicable for bone regeneration therapy.

Field of Study: Oral Biology   Student's Signature _____

Academic Year: 2015   Advisor's Signature _____

                                       Co-Advisor's Signature _____

ACKNOWLEDGEMENTS

จุฬาลงกรณ์มหาวิทยาลัย

CHULALONGKORN UNIVERSITY

CONTENTS

List of figures

จุฬาลงกรณ์มหาวิทยาลัย
CHULALONGKORN UNIVERSITY

List of tables

Chapter 1: Introduction

Periodontal ligament is a specialized fibrous connective tissue that spans the space between the alveolar bone and the cementum covering the root surface of teeth. It plays an essential role in supporting and maintaining the tooth in alveolar bone socket. Periodontal ligament fibroblasts (PDL cells) are, the most prominent cellular constituent of the periodontal ligament [1]. It has been suggested that periodontal ligament fibroblasts maintain their fibroblast-like characteristics by mechanical forces from occlusal loading [2]. Under physiological conditions, they are characterized by a high remodeling activity of the extracellular matrix, preventing the deposition of mineralized tissue. However, several studies have shown that when appropriately triggered, PDL cells can differentiate into either osteoblasts or cementoblasts [3, 4]. Upon stimulation, PDL cells exhibit numerous osteoblast-like properties including mineral deposition, bone-related gene expression such as alkaline phosphatase (*ALP*), osteocalcin (*OC*), and osteopontin (*OPN*) as well as a response to bone-inducing factors [3, 5-7]. The underlying mechanisms responsible for this plasticity of PDL cells are unknown. One possible mechanism might be related to epigenetics, since histone deacetylases (HDACs) have shown to play a role in osteoblast differentiation. Inhibition of HDAC activity was shown to accelerate osteoblastic differentiation *in vitro* in different cell types such as osteoblasts, bone marrow mesenchymal cells, and adipose-derived stromal cells [8-10].

In response to environmental, developmental, or metabolic cues, epigenetic regulates changes in gene expression and determines the cell's fate. Histone modification takes an important part in the regulation of chromatin structure.

Acetylation of histones provides a more open chromatin structure, which correlates with gene activation, while histone deacetylation results in transcriptional repression. These two phenomena are controlled by histone acetyltransferases (HATs) and histone deacetylases (HDACs), respectively [11]. To date, there are eighteen members of the human HDAC family which can be categorized into two groups based on Zn^{2+} and NAD^+-dependence. The Zn^{2+}-dependent subfamily includes the class I HDACs (HDAC 1, 2, 3, and 8) which are widely expressed in many cell types. Class IIa (HDAC 4, 5, 7, 9), class IIb (HDAC 6 and 10) and class IV (HDAC 11) are expressed in a more tissue-specific fashion [12].

The present study, we aim to evaluate the possible role of HDACs in the osteogenic differentiation of human PDL cells (hPDLs) using trichostatin A (TSA), a pan inhibitor of class I and II HDACs [13].

Research question

Does the inhibition of histone deacetylases enhance the osteogenic differentiation of hPDLs?

Objectives and hypotheses

Objective 1

To investigate the effect of an HDAC inhibitor on bone-associated gene expression in hPDLs during osteogenic differentiation.

Hypothesis

Inhibitor-treated cells express higher levels of bone-associated genes during osteogenic differentiation.

Experimental design

1.1   To determine the appropriate dose of an HDAC inhibitor (TSA), cell viability and proliferation of hPDLs were assessed by MTT assay. After seeding on a 24-well plate, the cells were supplied with various concentrations of TSA. The highest doses of TSA that do not decrease cell proliferation were selected for further experiments.

1.2   To assess the effect of an HDAC inhibitor on osteoblast-related gene expression, hPDLs were induced in osteogenic medium for different periods. After that, the mRNA was extracted for reverse transcriptase polymerase chain reaction (RT-PCR) analysis and/or real-time polymerase chain reaction for bone associated gene expression that of runt-related transcription factor 2 (*RUNX2*), osterix (*OSX*), type I collagen (*COL1*), alkaline phosphatase (*ALP*), bone sialoprotein (*BSP*), sclerostin (*SOST*), dentin matrix acidic phosphoprotein 1 (*DMP1*), dentin sialophosphoprotein (*DSPP*), osteocalcin (*OC*) and osteopontin (*OPN*).

1.3   Alkaline phosphatase activity, an early functional marker of osteoblast, was measured during osteogenic differentiation of hPDLs with or without TSA.

1.4   Deposition of mineral matrix was evaluated by both Von Kossa and Alizarin Red staining after inducing in osteogenic medium with or without TSA.

Objective 2

To verify whether inhibition of HDACs enhances osteogenic differentiation specifically, the effect of an HDAC inhibitor on adipogenic-associated gene expression in hPDLs during adipocyte differentiation.

Hypothesis

Inhibitor-treated hPDLs do not express characteristic of adipocyte after adipogenic differentiation.

Experimental design

2.1   To assess adipogenic differentiation, hPDLs were induced in adipogenic medium for different periods. mRNA was extracted for RT-PCR analysis of adipocyte-associated gene expression such as that of lipoprotein lipase (*LPL*) and peroxisome proliferator-activated receptor-γ 2 (*PPARγ2*).

2.2   Oil red O staining was used to determine adipocyte-like cells after inducing hPDLs in adipogenic medium with and without TSA.

Objective 3

To investigate the expression pattern of RUNX2, acetylated histone H3 and class I HDAC (HDAC 1, 2, 3); class IIa (HDAC 4), and class IIb (HDAC 6) in hPDLs during normal and osteogenic differentiation with or without inhibitor.

Hypothesis

Inhibitor-treated cells express higher levels of RUNX2, acetylated histone H3 and alter the levels of HDACs during osteogenic differentiation.

Experimental design

3.1   To examine whether HDAC inhibitor was able to alter the acetylation level of histone protein, we chose to observe Histone H3, which is one of the histone subunits important for regulating chromatin structure. Western blot analysis was conducted on lysates of hPDLs cultured in growth or osteogenic medium for different time period with and without inhibitor. The level of RUNX2, Histone 3 H3 and acetylated H3 protein were measured by immunoblotting. For non-histone protein, we performed immunoprecipitation with acetylated lysine and immunoblotting with RUNX2.

3.2   The level of HDAC 1, 2, 3, 4, 6 proteins were evaluated by Western blotting after culturing hPDLs in growth or osteogenic medium for different time periods with or without inhibitor.

Objective 4

To investigate the influence of an HDAC inhibitor on the osteogenic differentiation of hPDLs in a 3D culture model with a PCL/PEG scaffold and in a calvarial defect model in mice.

Hypothesis

Inhibitor-treated cells promote osteogenic differentiation in a 3D culture model with a PCL/PEG scaffold and in a calvarial defect model in mice.

Experimental design

4.1   To investigate the effect of TSA on osteogenic differentiation, 3D culturing in PCL/PEG scaffolds is performed. Alizarin Red and Von Kossa staining were used to assess amount of mineral formation.

4.2   To evaluate the efficacy of an HDAC inhibitor to promote bone regeneration *in vivo*, calvarial bone graft model was utilized in C57BL/6Mlac mice with a PCL/PEG scaffold, supplemented with hPDLs and TSA. After 4 and 8 weeks, the animals were sacrificed and the calvarial tissue will be harvested for histology sectioning and micro CT.

4.3   To confirm the survival of hPDLs in mouse calvarial and the effect of human cells on mouse immunity, immunohistochemistry and mouse serum IgG ELISA were performed.

Expected benefit

The knowledge gained from this study increase our understanding of the expression and the possible role of HDACs in osteogenic differentiation of hPDL. The application of HDAC inhibitors in bone regeneration can lead to a more effective therapy.

Research design

Laboratory experimental research

Conceptual framework
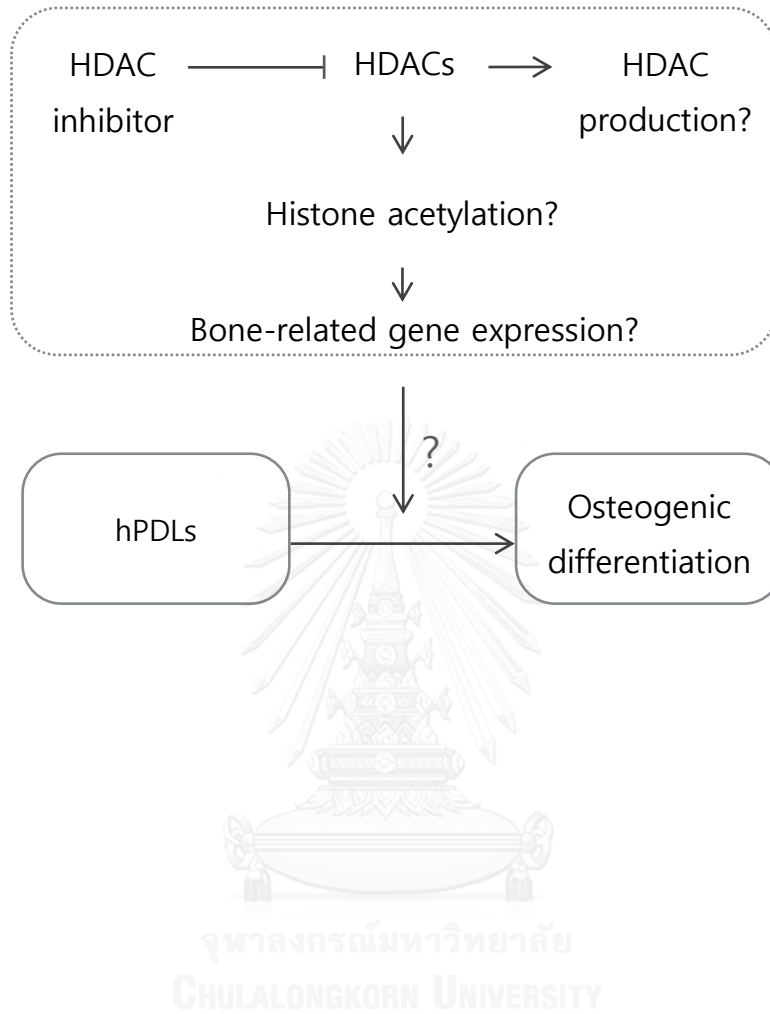
Chapter 2: Literature review

Epigenetics and histone acetylation

Epigenetics refers to the non-sequence-based structural changes of chromosomal regions that can alter the gene expression in response to external signals. Major types of epigenetic modifications include chromatin remodeling, DNA methylation, histone modifications and non-coding RNA. These components contribute to the regulation of crucial nuclear activities like DNA replication, repair and transcription. Hence, it plays an important role in stem cell maintenance and differentiation [14].

The basic molecular repeating unit of chromatin is a nucleosome, in which 145-147 bp of DNA is wrapped nearly twice around a histone octamer, containing two molecules of each histone H2A, H2B, H3, H4 and the linker histone H1 adjacent to the nucleosomes. The histones are required for folding to the higher-order chromatin structure. The chromatin structure is dynamic; loosely packed chromatin (euchromatin) is more accessible to the transcriptional apparatus leading to active gene expression, while tightly packed chromatin (heterochromatin) physically limits the access of the transcriptional machinery to DNA, leading to transcriptional inactivity [15]. This transition between the euchromatin and heterochromatin state is regulated by epigenetic processes such as chromatin-remodeling mechanisms including DNA methylation, histone acetylation, poly-ADP-ribosylation, and ATP-dependent chromatin remodeling. Acetylation is the only modification that directly causes a structural relaxation of chromatin by neutralizing charge of histones [16]. Other modifications act as docking sites that promote the recruitment and stabilization of effector protein complexes. The H3 and H4 core histone tails are the main targets

for acetylation and methylation, primarily at lysine and arginine residues. Methylation and acetylation of specific lysine residues on histones have defined roles in regulating gene expression. In general, the presence of histone modifications is involved in gene regulation [17, 18].

As considered, acetylation of histones provides a more open chromatin structure, which correlates with gene activation, while histone deacetylation results in transcriptional repression. There are several important positions for acetylation including Lys9 and Lys14 on histone H3, and Lys5, Lys8, Lys12 and Lys16 on histone H4, which are involved in the permissive chromatin structure [19, 20]. In general, there are three possible mechanisms, by which histone acetylation regulates transcription (Fig.2.1) [21]. Firstly, the phosphodiester backbone of the DNA is negative charge that is able interact potentially with the highly positive charge of the histones N-termini leading to a highly compacted chromatin. Acetylation of specific lysine residues within the histone tails could therefore serve to neutralize this positive charge leading to a loosening of histone–DNA interactions [16]. Furthermore, the acetylation pattern also serves as a signal that recruits certain chromatin or transcription-associated proteins called bromodomain to specifically read the signal. In general, bromodomain is an approximately 110 amino acid protein domain that recognizes acetylated lysine residues such as those on the N-terminal tails of histones. The recognition is often a prerequisite for protein-histone association and chromatin remodeling resulting the activation of transcription [22]. Lastly, when histone tails undergo different modifications (i.e. acetylation, methylation, phosphorylation and ubiquitination) in a combinatorial and consistent manner forming a code that is read by cellular machineries. This code is called "histone code" which is served as

chromatin-template beyond the genetic code of the DNA template [21, 23]. In detail, distinct histone amino-terminal modifications can generate synergistic or antagonistic interaction affinities for chromatin-associated proteins, which in turn dictate dynamic transitions between transcriptionally active or transcriptionally silent chromatin states. Thus, this code permits the assembly of different epigenetic states, leading to distinct outcomes of the genetic information, such as gene activation versus gene silencing or, more globally, cell proliferation versus cell differentiation [23].

Histone deacetylase

The acetylation and deacetylation of histones are controlled by histone acetyltransferases (HATs) and histone deacetylases (HDACs), respectively. HATs transfer an acetyl group from acetyl coenzyme A (acetyl-CoA) onto the ε-amino groups of conserved lysine residues within the core histones. Based on their suspected cellular origin and functions, HATs family is divided into two different classes. Type A HATs are located in the nucleus and are involved in the regulation of gene expression through acetylation of nucleosomal histones in the chromatin. While type B are located in the cytoplasm and are responsible for acetylating newly synthesized histones from the cytoplasm to the nucleus for deposition onto newly replicated DNA. Type A contains a bromodomain helping them recognize and bind to acetylated lysine residues on histone substrates. The acetyl groups added by type B to the histones are removed by HDACs once they enter the nucleus and are incorporated into chromatin [24].
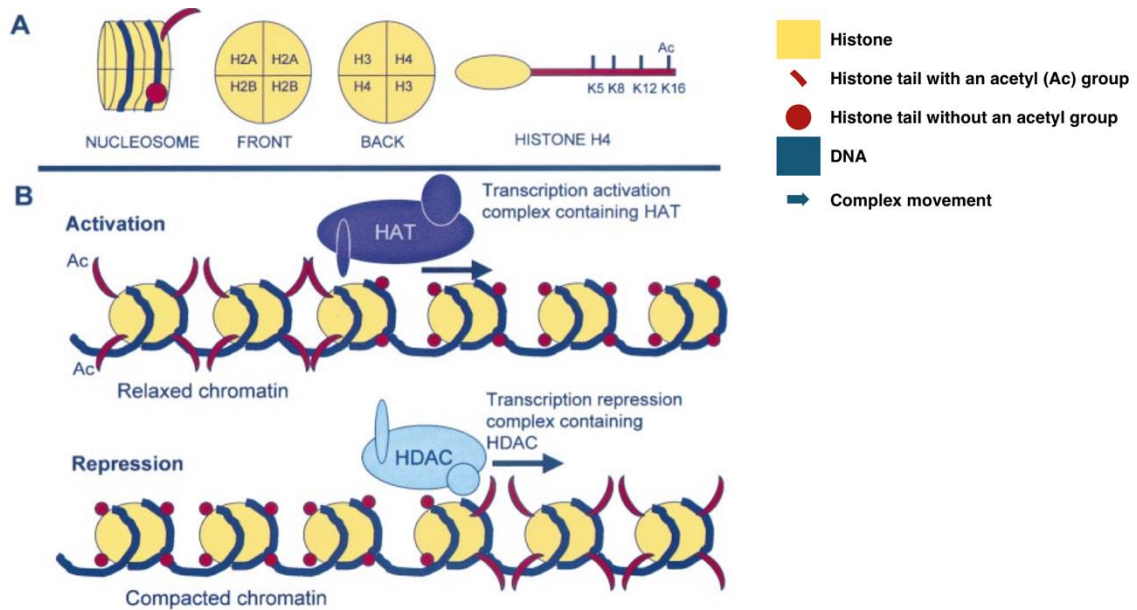
Figure 2.1: Nucleosome and histone acetylation. A) Schematic representation of a nucleosome. (B) Transcriptional repression and activation in chromatin. Both histone acetyltransferase (HAT; activation) and HDAC (repression) require several cofactors (for DNA binding, for recruitment of the complex, for remodeling of the DNA helix to reduce the accessibility of transcription factors) for their activity (adapted from [12]).

The eighteen members of the human HDACs family are divided into two groups based on Zn^{2+} and NAD^+-dependent deacetylases. The Zn^{2+}-dependent subfamily includes the class I HDACs (HDAC 1, 2, 3, and 8) that are widely expressed in many cell types. Class IIa (HDAC 4, 5, 7, 9), class IIb (HDAC 6 and 10) and class IV (HDAC 11) are expressed in a more tissue-specific fashion (Fig.2.2, Table 2.1). The subfamily of HDACs remove acetyl group from the histones comprising the nucleosome leading to histone hypoacetylation, which results in a decrease in the space between the histones and the DNA wrapped around it. On the

other hand, class III HDACs, which have homology to yeast Sir2, include sirtuins 1-7 and absolutely require NAD^+ for functioning. In addition to histone modification, some HDACs can act on non-histone proteins as well. Phylogenetic analysis of bacterial Zn^{2+} dependent HDACs suggests that they precede the evolution of histone proteins. This finding raises the possibility that the primary activity of some HDAC enzymes is directed against non- histone substrates [25]. For instance, using vorinostat to inhibit HDACs altered about 10% of acetylation sites in total 3600 lysine acetylation sites on 1750 proteins [26]. Lysine acetylation sites in proteins were proven to play an important role in diverse cellular processes, such as chromatin remodeling, cell cycle progression, splicing, nuclear transport, actin nucleation as well as in gene expression, RNA signaling, DNA damage repair, cytoskeleton function, protein chaperone, and ribosome formation and function [26, 27].

Class I HDACs: Expressed ubiquitously, class I HDACs have a simple structure including a conserved deacetylase domain and relatively short amino and carboxy terminal extensions. Uniquely, HDAC3 lacks a small segment corresponding to the extreme N termini of HDAC1, HDAC2, and HDAC8, suggesting a unique functions distinctly from other class I HDACs [28]. Combine with other transcription factors and co-repressors, class I establishes protein complexes such as mSin3 and Mi2 that play an important role in regulation of gene expression. For example, HDAC-mSin3 complexes can be recruited to transcriptional complexes including unliganded nuclear receptors, methyl CpG-binding protein 2 (MeCP2), and p53 [29, 30]. Studies showed that the purified endogenous HDAC 3 complex contains nuclear receptor corepressor (NCoR) and silencing mediator for retinoid and thyroid receptors (SMRT) proteins, and HDAC 3 appears to form the most stable complex in

comparison to other HDACs [28]. Through an association with the retinoblastoma (Rb) protein, class I HDACs also regulate cell cycle by binding the E2F transcription factor to repress transcription while knocking HDAC 1, 2, 3 leads to embryonic lethal *in vivo* [27, 29, 30].

Class II HDACs: Larger molecules than class I HDACs, class II display cell type-restricted patterns of expression and have conserved binding sites for human myocyte enhancer factor 2 (MEF2) transcription factors and the 14-3-3 chaperone proteins, which are involved in regulation of the shuttling of these enzymes between the nucleus and cytoplasm [29, 30]. Specially, HDAC4 has a central role in the formation of the skeleton. Expressed in prehypertrophic chondrocytes, HDAC 4 regulates chondrocyte hypertrophy and endochondral bone formation. It interacts with Runx2 and inhibits the activity of this transcription factor. Moreover, HDAC4-null mice display premature ossification of developing bones [31]. On the other hand, HDAC 5, 7, 9 involve in cardiac and vascular endothelial functions [32].

Different from other the Zn^{2+} dependent HDACs, HDAC 6 has two catalytic sites and one ubiquitin binding site toward the C-terminus. Recognized as a tubulin-deacetylase, mice lacking HDAC 6 are viable although they have highly elevated tubulin acetylation in multiple organs [32]. The ubiquitin site toward the C-terminal end of HDAC6 plays a critical role in aggresome formation in the pathway of proteolysis of misfolded proteins [30]. There is a little knowledge about the function of HDAC10. It has a bipartite structure consisting of an N-terminal catalytic domain and a C-terminal leucine-rich domain. The leucine-rich domain is responsible for cytoplasmic enrichment of HDAC 10 [33].

Class IV HDAC: Found recently, HDAC 11 is the only member of class IV HDAC which has characteristics of both class I and class II. In antigen presenting cells, HDAC 11 negatively regulates expression of interleukin-10 leading to prime naive T cells and restore the responsiveness of tolerant CD4+ T cells. Conversely, disruption of HDAC11 in these cells caused the upregulation of IL-10 and impairment of antigen-specific T cell response These findings suggest that HDAC11 has molecular targets that influence immune function [34].

Class	Protein domains		Time of lethality	Phenotype
Class I	HDAC1	S S — 482	E10.5	Proliferation defects
	HDAC2	S S — 488	P1	Cardiac malformation
	HDAC3	S — 428	E9.5	Gastrulation defects
	HDAC8	S — 377	P1	Craniofacial defects
Class IIa	HDAC4	MEF2 14-3-3 14-3-3 14-3-3 S S S — 1,084	P7–P14	Chondrocyte differentiation defect in growth plate
	HDAC5	S S S — 1,122	Viable	Exacerbated cardiac hypertrophy after stress
	HDAC7	S S S S — 912	E11	Endothelial dysfunction
	HDAC9	S S S — 1,069	Viable	Exacerbated cardiac hypertrophy after stress
Class IIb	HDAC6	ZnF — 1,215	Viable	Increased tubulin acetylation
	HDAC10	Leucine rich — 669	ND	–
Class IV	HDAC11	— 347	ND	–

Conserved HDAC domain
482, 488… Number of amino acids
Myocyte enhancer factor 2 (MEF2)-binding sites
14-3-3 14-3-3 chaperone protein binding sites

Figure 2.2: Schematic representation of Zn^{2+}-dependent HDAC structure showing protein domains, loss-of-function phenotypes mice and time point of lethality of the knockouts. E: embryonic day, ND: not determined, P: days postnatal, S: serine phosphorylation sites, ZnF: zinc finger (adapted from [27]).

Table 2.1: Summary of Zn^{2+} dependent HDACs subfamilies (modified from Suzuki 2009 [35] and Marks 2010 [30]).

HDAC	Localization	Size (AA)	Chromosomal site (human)	Tissue distribution	Biologic functions*
Class I					
HDAC 1		483	1p34.1		Transcriptional repression; Cell survival, proliferation and differentiation
HDAC 2	Nucleus	488	6p21	Ubiquitous	
HDAC 3		423	5q31		
HDAC 8		377	Xq13		Smooth muscle cell contractility
Class IIa					
HDAC 4		1048	2q372	H, SM, B	Transcriptional repression; Chondrocyte and osteocyte development differentiation; Muscle differentiation block Retinal protection
HDAC 5	Nucleus/ Cytoplasm	1122	17q21		Transcriptional repression; Muscle differentiation block; Myocardium, endothelial
HDAC 7		855	12q13	H, PL, PA, SM	Transcriptional repression; Muscle differentiation block; Thymocyte differentiation
HDAC 9		1011	7p21–p15	SM, B	
Class IIb					
HDAC 6	Mainly cytoplasm	1215	Xp11.22–33	H, L, K, PA	Targets tubulin, chaperones, etc.
HDAC 10		669	22q13.31–33	L, S, K	Unknown
Class IV					
HDAC 11	Nucleus/ Cytoplasm	347	3p25.2	B, H, SM, K	Transcriptional repression; Immunomodulators

SM—skeletal muscle; B—brain; PL—platelet; L—liver; K—kidney; S—spleen; H—heart; PA—pancreas.
* The biological functions of the different HDACs are not completely understood.

Histone deacetylase inhibitor

Inhibition of HDACs can result in a general hyperacetylation of histones leading to the relaxation of the DNA compaction, which is followed by the transcriptional activation. To inhibit HDACs by blocking access to the active site, a number of natural and synthetic inhibitors have been identified. Typically, a HDAC inhibitor contains common structural characteristics including: a zinc-binding group (ZBG) which coordinates the zinc ion in the active site, a cap substructure which interacts with amino acids at the entrance of the N-acetylated lysine binding channel of HDAC, and a linker connecting the cap and the ZBG at a proper distance (Fig.2.3) [35].

Forming by a stretch of about 390 amino acids with a set of conserved amino acids, the catalytic domain of HDAC consists of a gently curved tubular pocket. A Zn^{2+} ion is bound to the zinc binding site at the bottom of this pocket. This atom is an essential component of the charge-relay system, which facilitates hydrolysis of the acetyl-lysine bond during the removal of the acetyl group from histone. HDAC inhibitors function by displacing the zinc ion and thereby rendering the charge-relay system dysfunctional. The inhibitors can be divided into several structural classes including hydroxamates, cyclic peptides, aliphatic acids, and benzamides (Table 2.2) [12].

One of the most potential inhibitor is Trichostatin A (TSA) with a hydroxamic acid group and five-carbon atom linker to the phenyl group. The structure makes TSA optimal in conformation to fit into the active site of HDACs. HDACs both class I and II are thought to be approximately equally sensitive to inhibition by TSA. HDAC inhibitors can cause the accumulation of acetylated histones and other non-histone proteins that alter the structure of many proteins targets of HDACs leading to the

regulation of gene expression, cell proliferation, cell migration, and cell death. However, the exact mechanisms are not fully understood [12]. Because of the effect in cellular function regulation, many studies showed that HDAC inhibitor can cure cancer, inflammation, nerve degradation or learning and memory enhancing after brain injury [32, 36-39]. Some of the compounds mentioned above have been entered into clinical trials such as NaB, SAHA, phenylbutyrate, depsipeptide, pyroxamide, valproic acid (VPA). In couple with pan-inhibitors which act on many HDAC members leading to wide range of effects in patients, a number of selective HDAC inhibitors are effortfully studied that would be advantageous for specific clinical use [32].
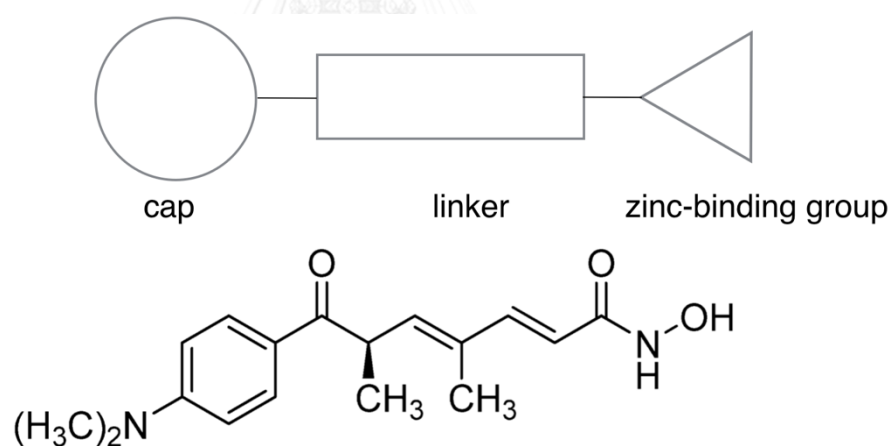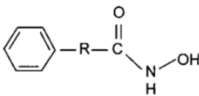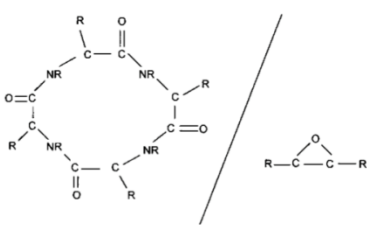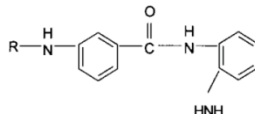
Figure 2.3: Structural characteristics of HDAC inhibitors and the structure of Trichostatin A (TSA). The CO and OH groups are thought to chelate the zinc ion in the active site of HDAC in a bidentate fashion (modified from [35]).

Table 2.2: The features of four groups of HDAC inhibitors [12].

Group and structure	Compounds	*In vitro* IC_{50} range
Hydroxamic acids	TSA	nM
	Suberoyl anilide bishydroxamide (SAHA)	μM
	M-carboxycinnamic acid bishydroxamide (CBHA)	μM
	Scriptaid	μM
	Pyroxamide	μM
	Oxamflatin	nM
Short-chain fatty acids	Butyrate	mM
	Phenylbutyrate	mM
	Valproic acid	mM
Cyclic tetrapeptides/epoxides	Trapoxin	nM
	HC-toxin	nM
	Chlamydocin	nM
	Depudesin	μM
	Apicidine	nM–μM
	Depsipeptide (FK228)	nM
Benzamides	*N*-acetyldinaline (CI-994)	μM
	MS-275	μM

Histone deacetylase and osteogenic differentiation

Bone, which is mesenchyme in its origin, is a tissue that consists cells, fibers, extracellular matrix and inorganic component. It has the potential to repair itself throughout the life via the coordinated function of several cell types including bone forming cells (osteoblasts), bone resorbing cells (osteoclasts), and quiescence osteoblasts (osteocytes). While osteoclasts are derived from the hematopoietic lineage and have a role in bone resorption, osteoblasts are derived from multipotential stem cells which are termed stromal stem cells, mesenchymal stromal cells, skeletal stem cells, stromal fibroblastic stem cells, and most recently, mesenchymal stem cells. These cells are driven into osteoprogenitors and thereafter osteoblasts which are located on the surfaces of bone and synthesized osteoid matrix [40, 41].

During the formation of bone, Wingless-int (WNT/β-catenin) and transforming growth factor -β/bone morphogenetic protein (TGF-β/BMP) pathways modulate key transcriptional factor RUNX2 to induce the osteogenic phenotype. RUNX2, which is a crucial key for osteoblast development, induces and starts a cascade of serial expression of other transcription factors and bone-specific genes. One of the important downstream transcription factors of RUNX2 is OSX. Although OSX transcription is positively regulated by RUNX2 and in the absence of Osx, osteoblasts also do not form, the regulation of OSX is still poorly understood. Generally, Wnt/β-catenin directs osteoblast differentiation at the preosteoblast stage leading to the up-regulation of RUNX2 expression and increase its promoter activity. RUNX2 is required for mesenchymal progenitor cell differentiation into preosteoblasts, and for suppressing their differentiation into adipocytes and chondrocytes. OSX and Wnt/β-catenin also direct the differentiation of preosteoblasts

into immature osteoblasts and with the potential abolishment into chondrocytes. The activity of RUNX2 is limited by TWIST proteins. Their expression ceases the Runx2-mediated differentiation of osteoblast lineage. Some other important transcriptional activators, such as Activator protein 1 (AP1), Special AT-rich sequence-binding protein 2 (Satb2), and Activating transcription factor 4 (ATF4) are also required for proper osteoblast proliferation, differentiation and bone matrix deposition [40, 42, 43].

Based on observations of *in vivo* studies and in bone nodule formation *in vitro*, the osteogenic differentiation could be divided into three distinctive stages: proliferation, extracellular matrix development and maturation, and mineralization (Fig.2.4). Each stage is featured with characteristic changes in gene expression. Begin with *COL1*, the sequential up-regulation of bone-related gene expression is followed by *ALP, BSP*, and finally *OCN*. Other matrix proteins, such as *OPN, DMP1, DSPP, SOST* increase once the osteoblasts begin to transform into osteocytes. However, their expression is up-regulated asynchronously, acquired, and/ or lost as the progenitor cells differentiate and the matrix matures and mineralizes. These expressions are also various and reflect the inherent differences in the cellular populations, for example species differences, or different mixtures of more-or-less primitive progenitors and more mature cells because of the different parts of collected bone and tissue [44].

Decreasing proliferative capacity – increasing differentiation

→

Unlimited self-renewal (asymmetric divisions)	Limited self-renewal (asymmetric and/or symmetric divisions); extensive proliferation	Limited proliferation	Post-mitotic

Mesenchymal stem cells → Immature / Mature Osteoprogenitors → Preosteoblasts → Osteoblasts → Osteocytes

Requires stimulus, e.g. Dex → Default differentiation *in vitro*

	MSC	Immature OP	Mature OP	Preosteoblasts	Osteoblasts	Osteocytes
Transcription factors						
Runx2	+?	+	+	+	+	+
Osx	–	–	–	+	+	+
Enzymes						
ALP	–	–	+	++	+++	–
Phex	–	–	–	–	++	+++
Extracellular matrix						
ColII	–?	–	+	++	+	–
OPN	+?	–/+	–/+	– → +	– → +++	– → +++
BSP	–	–	++	– → +++	– → +++	– → +++
OCN	–	–	–	–	– → +++	–
Factors and receptors						
PTH1R	?	–	–/+	++	++	++
PTHrP	?	–/+	+	++	++	–
PDGFRα	?					
Sclerostin	–	–	–	–	–	+++
DMP1	–	–	–	–	–	+++

-      no detectable expression;
- –□/+ to +++   expression ranging from detectable to very high;
- ?   intercellular heterogeneous expression.

Figure 2.4: Suggested sequential proliferation–differentiation steps of several well-established markers in the osteoblast lineage as detectable from *in vitro* and *in vivo* experiments. Dex, Phex, PTH1R, PTHrP, PDGFRα [40].

As discussed, epigenetics including histone acetylation play an important role in cell proliferation and differentiation. Hence, this histone modification also regulates osteogenesis process in mesenchymal cells. Studies showed that the acetylated histone H3 and H4 proteins are associated with the OC promoter only when the gene is

transcriptionally active. The results suggest functional linkage of H3 and H4 acetylation in specific regions of the OC promoter to chromatin remodeling that accompanies tissue-specific transcriptional activation [45, 46]. Most post-translational histone modifications are dynamic and regulated by families of enzymes that promote or reverse specific modifications such as HATs and HDACs, which control the acetylation, and histone methylases and demethylases, which control the methylation. Several HDACs have been identified as regulators of osteoblastic differentiation and maturation (Fig.5) [31, 47, 48]. Westendorf et al. showed that HDAC 6 represses the p21 promoter in immortal fibroblasts [47]. HDAC 1 and 3 are transcriptional co-repressors of osteoblastic differentiation by interacting with a bone-related transcription factor, RUNX2, to modulate its downstream genes like osteocalcin [49, 50]. HDAC 1, 2 and 8 have been reported to be down-regulated during osteogenenic differentiation of osteoblasts, bone marrow stem cells and dental pulp cells [48, 51, 52]. Taking together, these data indicate that inhibition of individual HDACs is sufficient to promote osteoblast differentiation but different HDAC complexes might have distinct roles during the process.

HDAC 4 was reported to regulate chondrocyte hypertrophy and endochondral bone formation by interacting and inhibiting the activity of RUNX2 [31]. Lu et al. showed the abnormal expression of HDAC4 in osteoarthritic cartilage. This finding might implicate in promoting catabolic activity of chondrocyte, which is associated with osteoarthritic pathogenesis. Additionally, decreased HDAC4 was associated with increased RUNX2 and other osteoarthritic-related genes in human osteoarthritic cartilage while over-expression of HDAC4 had an opposite effect [53, 54]. More experiments are needed to understand the roles of all HDACs in chondrocytes.

It is poorly understood about the role of HDACs in osteoclasts. HDAC 1 is recruited to the promoters of important osteoclast genes including NFATc1 and osteoclast-associated receptor (OSCAR) to regulate their expression and inhibit osteoclast maturation [55]. Rho activity and HDAC6 regulate acetylated microtubule levels in osteoclasts which increase during osteoclast maturation [56]. Suppression of HDAC 3 expression by shRNA or inhibitors inhibits osteoclast differentiation, whereas suppression of HDAC 7 expression accelerated osteoclasts differentiation. The study indicated that the transcriptional activity of Mitf, a transcription factor necessary for osteoclast differentiation, is repressed by HDAC 7 [57]. In addition, upon RANKL activation, HDAC 7 suppresses NFATc1 and prevents β-catenin down-regulation, thereby blocking osteoclast differentiation [58].
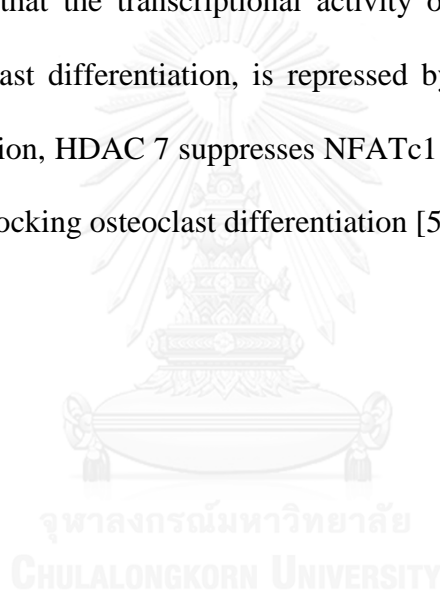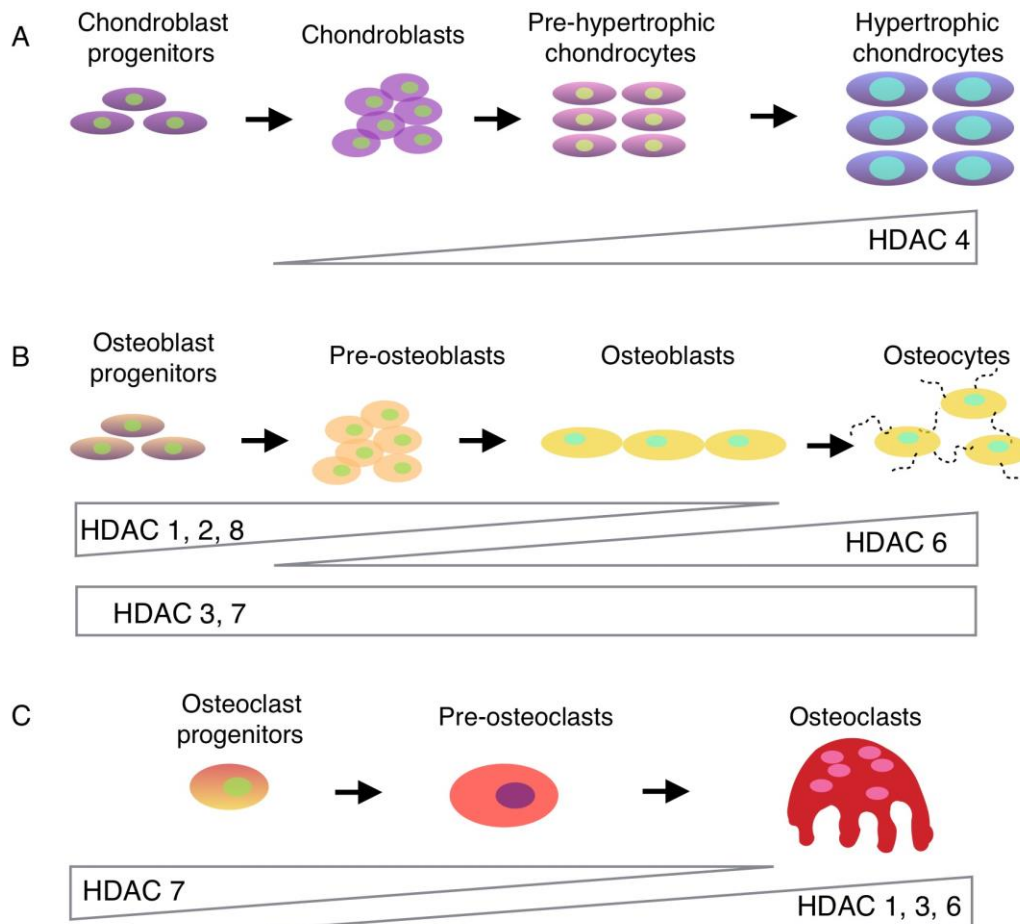
Figure 2.5: Suggested expression fashion of HDACs in A) chondrocyte, B) osteoblast, and C) osteoclast maturation (modified from [59] with references from [31, 48-52, 55-57]).

Up to date, HDAC inhibitors are used in clinical trials to cure several diseases. The inhibitors are also considered in bone related therapies such as tissue engineering for bone regeneration. However, there are conflicting reports regarding the different effect of HDAC inhibitors between *in vitro* and *in vivo* data. While *in vitro* studies showed that HDAC inhibitors promote differentiation, *in vivo* results indicate the decrease in bone mineral density in patients with osteogenic therapy [60]. More studies are needed to elucidate the precise functions of HDACs and possible side

effects of the inhibitor. Long term administration should be approached with carefulness.

PCL/PEG scaffold and mouse calvarial defect model

Tissue engineering originates in reconstructive surgery, a field that involves the replacement of organs to repair the function of damaged tissue. Bone graft substitutes, in the concept of bone tissue engineering, is referred as materials used to form/replace bone in various part of the body. Recent technology mainly focused on improving the osteogenic potential of bone grafting materials either by incorporating osteoprogenitor cells or growth factors into a scaffold made of various materials, which mimic the bone microenvironment [61]. To be compatible with the natural structure of bone, scaffolds should have a specific three-dimensional (3-D) shape, high porosity, a fully interconnected geometry, a large surface area, and structural strength [62]. Polycaprolactone (PCL) is a semi-crystalline polyester that is degraded by the hydrolysis of its ester linkages under physiological conditions. The degradation of PCL and its copolymers with a high molecular weight ($\geq$50,000 g/mol) is remarkably slow, requiring 3 years for complete removal from the host body [63]. This polymer has received FDA approval and is already used in drug delivery devices, sutures, and adhesion barriers. Additionally, due to its excellent biocompatibility, mechanical strength, lack of toxicity, and low cost, PCL is one of the biodegradable polyesters that has attracted the most attention in bone tissue engineering. 3D PCL scaffolds with highly porous and interconnected networks can be prepared using modified solvent casting, particulate leaching, and polymer leaching techniques, which implement sodium chloride and polyethylene glycol (PEG) as porogens [64].

In vivo research with animal models has been a preferred experimental system in bone-related biomedical research since, by approximation, it provided relevant data gathering regarding physiological and pathological conditions that could be of use to establish more effective clinical interventions. Moreover, bone tissue is characterized by an adequate capacity to regenerate itself following the establishment of a lesion or a defect, when the physiological stimuli converge to establish a proper response. The calvarial model stands out as an adequate model for evaluating complex materials and tissue engineering constructs aiming bone regeneration, especially which refers to the regeneration of craniofacial defects. The calvarial bone structure allows the establishment of a uniform, reproducible and standardized defect that is easily evaluated by radiographic and histological analysis; the anatomic location reflects an adequate size for surgical access and intraoperative handling [65]. In term of calvarial defect, critical-sized calvarial defect (ASC) in the mouse is a reproducible, frequently utilized model for the study of cell-based skeletal repair. Studies have demonstrated that there was no spontaneous healing of a critical sized (4mm, parietal bone) mouse calvarial defect demonstrated without ASC engraftment up to 16 weeks post injury [66]. In addition, it had been proven in the literature that the calvarial bone defects in mice whose diameters exceed 2.7mm are considered critical while defects smaller than 1.8mm in diameter were shown to heal spontaneously with a maximum healing rate of 50% within a year postoperatively [67, 68].

Chapter 3: Materials and Methods

Isolation and culture of the primary human PDL cells

hPDLs were cultured and characterized as our previous study [69]. Third molars from healthy young individuals, age 18 to 25 year-old, were extracted as recommended by their dentist and with informed consent of the patient. Each subject was without systemic and oral infection or diseases and the molars had no caries. Immediately after extraction, each tooth was transferred in ice cold storage medium (10% FBS, 1% L-Gluamine, 0,5 mg/ml gentamicin and 3 mg/ml amphotericin B in DMEM, #11960, Gibco, Life Technologies Corporation, Grand Island, NY, USA) on ice and sent to the lab. To avoid contamination, the soft tissue attached to the cervical area was carefully removed. The extracted molars were rinsed twice in Dulbecco's phosphate-buffered saline without calcium and magnesium (PBS). Then the periodontal ligament attached to the root surface of the middle one-third was scraped off the surface with a surgical blade and minced into 2 x $2mm^2$ pieces. The tissue explants were seeded in culture medium (10% FBS, 1% L-Gluamine, 1% antibiotics in DMEM, Gibco) until outgrowing cells reached confluence. The cells were incubated at 37°C humidified atmosphere with 5% CO2, the medium was replaced every 3 days. The primary human PDL cells at the 3rd–8th passage were used for the following experiments. The patients provided written consent for the use of discarded tissues for research purposes. Tissue samples were deidentified and analyzed anonymously. The Ethics Committee of the Faculty of Dentistry, Chulalongkorn University, Thailand has approved the study to be carried out according to the protocol and informed

permission dated and/or amended as follows in compliance with the ICH/GCP (HREC-DCU 2015-036).

Cell viability assay and morphology

The viability of hPDLs incubated with TSA was determined by using 3-(4,5-dimethylthiazol-2-yl)-2,5-diphenyl tetrazolium bromide (MTT; #298-931, USB Corporation, Cleveland, OH, USA) assay. The cells were plated in 24-well plate at 2×10^4 cells/cm^2 in culture medium. After 24 hr, the medium was changed to serum-free medium for 4 hours and then the cells were incubated with 50, 100, 200, 400, 800 nM TSA (#9950S, Cell Signaling Technology, Danvers, MA, USA) or vehicle (0.4% DMSO) for 72 hr in growth medium and osteogenic medium. The used concentrations of TSA corresponded to the manufactory's recommendation and to the concentrations used previously by others [8, 70]. The control group was cultured with the vehicle. After 72 hr, the medium was replaced with 0.5 ml MTT solution and incubated for 30 min at 37°C. The formazan product was dissolved in solubilization/stop solution. Using a microplate reader, the optical densities were measured at 570 nm. A different plate but employing the same protocol was used to observe cell morphology under inverted microscope (Nikon Eclipse TS100, Japan).

***In vitro* differentiation assay**

In vitro differentiation to osteogenic and adipogenic lineage was performed as follows. Briefly, hPDLs were initially cultured in growth medium. After confluence, the media were replaced by osteogenic or adipogenic medium; in the presence or absence of the HDAC inhibitor. The cells were cultured in adipogenic medium

(DMEM supplemented with 10% FBS, 1 μM dexamethasone, 200μM indomethacin, 10μg/ml insulin, and 0.5 mM isobutylmethylxanthine) for 7 and 21 days. The 21 days cultures were used for oil red O staining. To induce osteogenic differentiation, the cells were incubated in osteogenic medium (DMEM supplemented with 10% FBS, 50 μg/ml L-ascorbate-2-phosphate, 0.25 μM dexamethasone and 5 mM β glycerophosphate) for 3, 5 and 10 days. Mineral deposition was analyzed staining with Von Kossa and Alizarin red.

RNA preparation, semi-quantitative and real time reverse transcription–polymerase chain reaction (RT-PCR)

To assess the expression of osteoblast- and adipocyte-related genes by hPDLs and the effect of the HDAC inhibitor hereupon, semi-quantitative and real-time RT-PCR were performed. After incubation with and without TSA for 3, 5, 10 day in osteogenic medium or 7 days in adipogenic medium, total mRNA was isolated by using Trizol reagent (#2302700, Prime, Gaithersburg, MD, USA). The cells were scraped off the plate and collected. The lysate was extracted by adding 100 μl chloroform, mixed and centrifuged for 15 minutes at 14,000 rpm. mRNA was precipitated with 250 μl isopropanol and the pellet was dissolved in nuclease free water (DEPC). The amount of RNA was measured using a spectrophotometer (NanoDrop2000, Thermo Scientific, Wilmington, DE, USA). First-strand cDNA was synthesized using reverse transcriptase reaction by ImProm-II Reverse Transcription System (#A3800, Promega Corporation, Madison, WI, USA) and semi-quantitative PCR was performed as our previous studies [71, 72].

Semi-quantitative PCR was performed using Tag polymerase (Tag DNA Polymerase, Invitrogen, Thermo Fisher Scientific) with a reaction volume of 25 μl containing 25 pmol of primers and 1 μl of RT product. The amplification profile was one cycle at 94°C for 1 min, hybridization at 60°C for 1 min and extension at 72°C, followed by 1 extension cycle of 10 min at 72°C. The PCR was performed in the DNA thermal cycler (Biometra GmH, Germany) and subsequently the amplification cycle was repeated 22 –40 times. The cycle number was determined so that the PCR product levels were within a linear range. The amplified DNA was then electrophoresed on a 1.8% agarose gel and visualized by ethidium bromide (EtBr; Bio-Rad, Singapore) fluorostaining. PCR primer for runt-related transcription factor 2 (*RUNX2*), osterix (*OSX*), type I collagen (*COL1*), alkaline phosphatase (*ALP*), bone sialoprotein (*BSP*), sclerostin (*SOST*), dentin matrix acidic phosphoprotein 1 (*DMP1*), dentin sialophosphoprotein (*DSPP*), osteocalcin (*OC*), osteopontin (*OPN*) (Sigma-Aldrich) were used to screen the osteoblast-related genes, and lipoprotein lipase (*LPL*), and peroxisome proliferator-activated receptor-γ 2 (*PPARγ2*) were used as adipogenic differentiation markers (Table 3.1). All bands were scanned, analyzed, and normalized with the expression of the housekeeping gene glyceraldehyde 3-phosphate dehydrogenase (*GAPDH*) using Bio-1D software version 15.03 (Vilber Lourmat, Marne La Vallée, France). Quantitative real-time RT-PCR was performed to confirm differences in osteoblast-related gene expression utilizing LightCycler1 480 SYBR Green I Master kit (#06402712001, Roche Diagnostics GmH, Mannheim, Germany) and real time thermal cycler (Bio-Rad). The threshold cycle (CT) for each sample was calculated using the real-time cycler software and change from CT to fold change of

genes by Bio-Rad CFX 2.1 manager software. Three independent experiments were repeated in each sample.

Table 3.1: PCR primer sequences.

Primer	Gene ID	Sequences (Forward and Reverse 5'-3')	Size (bp)	Cycles
ALP	NM_000478.4	F: CGA GAT ACA AGC ACT CCC ACT TC R: CTG TTC AGC TCG TAC TGC ATG TC	121	35
BSP	NM_004967.3	F: GAT GAA GAC TCT GAG GCT GAG A R: TTG ACG CCC GTG TAT TCG TA	514	38
Q-BSP	NM_004967.3	F: ATG GCC TGT GCT TTC TCA ATG R: AGG ATA AAA GTA GGC ATG CTT G	123	
COL-1	NM_000088.3	F: GCA AAG AAG GCG GCA AA R: CTC ACC ACG ATC ACC ACT CT	500	22
Q-COL-1	NM_000088.3	F: GTG CTA AAG GTG CCA ATG GT R: ACC AGG TTC ACC GCT GTT AC	128	
DMP-1	NM_004407.3	F: CTG GGC TCT GAT GAT CAT CA R: TCA AGC TCG CTT CTG TCA TC	623	38
Q-DMP-1	NM_004407.3	F: ATG CCT ATC ACA ACA AAC C R: CTC CTT TAT GTG ACA ACT GC	100	
DSPP	NM_014208.3	F: TCA CAA GGG AGA AGG GAA TG R: TGC CAT TTG CTG TGA TGT TT	182	40
Q-DSPP	NM_014208.3	F: ATA TTG AGG CTG GAA TGG GG A R: TTT GTG GCT CCA GCA TTG TCA	136	
GAPDH	NM 002046.3	F: TGA AGG TCG GAG TCA ACG GAT R: TCA CAC CCA TGA CGA ACA TGG	396	22
Q-GAPDH	NM_002046.4	F: CAC TGC CAA CGT GTC AGT GGT G R: GTA GCC CAG GAT GCC CTT GAG	121	
LPL	NM_000237.2	F: GAG ATT TCT CTG TAT GGC ACC R: CTG CAA ATG AGA CAC TTT CTC	276	38
OC	NM_199173.2	F: ATG AGA GCC CTC ACA CTC CTC R: GCC GTA GAA GCG CCG ATA GGC	294	35
Q-OC	NM_199173.4	F: CTT TGT GTC CAA GCA GGA GG R: CTG AAA GCC GAT GTG GTC AG	166	
OPN	NM_00104006 0.1	F: AGT ACC CTG ATG CTA CAG ACG R: CAA CCA GCA TAT CTT CAT GGC TG	321	30
Q-OPN	NM_00104006 0.1	F: AGG AGG AGG CAG AGC ACA R: CTG GTA TGG CAC AGG TGA TG	150	
OSX	NM_00117346 7.1	F: GCC AGA AGC TGT GAA ACC TC R: GAC AGC AGG GGA CAG AAA AG	510	32
PPARγ2	NM_015869.4	F: GCT GTT ATG GGT GAA ACT CTG R: ATA GGT GGA GAT GCA GGC TC	351	38
RUNX2	NM_00102463 0.2	F: CCC CAC GACAAC CGC ACC AT R: CAC TCC GGC CCA CAA ATC	289	26
SOST	NM_025237.2	F: ACT TCA GAG GAG GCA GAA ATG G R: CAA GGG GGA ATC TTA TCC AAC TTT C	115	38

Alkaline phosphatase activity assay

ALP activity of hPDLs was measured with alkaline phosphate yellow liquid. In this reaction, ALP catalyzes the hydrolysis of a colorless organic phosphate ester substrate (p-nitrophenyl phosphate – PNPP, #002201, Invitrogen, Life Technologies Corporation) to yield a yellow product (p-nitrophenol) and phosphate. ALP activity of hPDLs during osteogenic differentiation was measured after 3, 5, 10 days. Briefly, cell lysates were collected by ALP lysis buffer (10 mM Tris-HCl pH 10, 2 mM MgCl$_2$, 0.1% Triton X-100) and the samples were scraped and frozen at -20 °C for 30 min before proceeding. For each well, 10 µL of 0.1 M amino propanol was mixed with 100 µL of 2 mM MgCl$_2$ following by adding PNPP at a concentration of 2 mg/mL. The solution (110 µL) was added to the sample and incubated at 37 °C for 15 min. The reaction was stopped with the addition of 900 µL/well of 50 mM NaOH. The extracted solution was placed in the UV-visible spectrophotometer; the absorbance was measured at 410 nm. The amount of yellow product was evaluated against a standard curve.

For the protein assay, the samples were treated in the same manner as in the ALP assay until the specimens were frozen. After freezing, bicinchoninic acid (Pierce BCA protein assay kit, Thermal Scientific, Rockford, IL, USA) solution was added to the specimens. The specimens were incubated at 37 °C for 15 min. The absorbance of the medium was then measured at 562 nm with the UV–visible spectrophotometer, and the amount of the total protein was calculated against a standard curve. To calculate ALP activity in the cells, amount of ALP activity product was normalized to total protein content and compared between groups.

Western blot analysis

Western blot analysis was conducted on cell lysates of cells cultured in control or osteogenic medium for 3, 5 and 10 days, with and without the inhibitor. Protein lysates were prepared by incubating the cells on ice in 0.5 mL RIPA buffer (150 mM NaCl, 1% NP40, 0.5% deoxycholate, 0.1% SDS, 50 mM Tris; pH 8.0) with protease inhibitor cocktail (#11697498001, Roche Diagnostics GmbH, Mannheim, Germany). The Pierce BCA protein assay (Thermal Scientific) was used to determine the protein concentration. 20 µg of the total protein was used for electrophoresis on a 10% denaturing polyacrylamide gel and transferred to a nitrocellulose membrane electrophoretically. To block nonspecific binding to proteins, membranes were incubated in Tris-buffered saline and tween 20 (TBS-T) containing 5% non-fat dry milk for 1 hr at room temperature. Overnight incubation was performed with primary antibodies raised against RUNX2 (#AF2006, R&D Systems, Minneapolis, MN, USA), HDAC 1, 2, 3, 4, 6 (#9928, Cell Signaling Technology) and β-ACTIN (#MAB1501, Merck Millipore, Darmstadt, Germany) with 1:1000 dilution in 5% skim milk. Follow by three times washing in TBS-T, the membranes were incubated with anti-goat IgG biotin conjugate (#B7014, Sigma) and HRP-Streptavidin Conjugate (#43-4323, Invitrogen) with 1:1000 dilution, or horseradish peroxidase-conjugated secondary antibodies (#7074, #7076, Cell Signaling Technology, 1:2000 dilution) for 1 h, then exposed to CL-Xposture film (Pierce, Thermal Scientific). Band density was quantified by Bio-1D.

For histone extraction, EpiQuik™ Total Histone Extraction Kit (#OP-0006, Epigentek, Farmingdale, NY, USA) was used to collect total histone. Histones were run in 15% denaturing polyacrylamide gel and transferred to PVDF membrane

electrophoretically. Then western blotting was performed with polyclonal antibody against histone H3 (#ab1791, Abcam, Cambridge, UK, 1:5000 dilution), acetyl histone H3 (#06-599, Merck Millipore, 0.05 µg/ml) with 10 µg total histone protein. Baseline of HDACs, histone H3 protein and acetyl H3 expression were examined in cells cultured in growth medium with or without inhibitor for 2 days.

Immunoprecipitation

To assess the acetylation of Runx2 protein, after appropriate treatments without and with 400nM TSA in growth and osteogenic media for 2 days, the cells were washed with ice- cold PBS twice and lysed in HEPES lysis buffer containing 25 mM HEPES pH 7.5 (#H-9136, Sigma), 150 mM NaCl, 10 mM sodium butyrate, 1% Nonidet P-40, 0.25% sodium deoxycholate, 10% glycerol supplemented with protease and phosphatase inhibitors (#05892791001, #04906845001, Roche Diagnostics GmbH). After assessing protein concentration, 500 µg (1µg/µl) protein from each sample was used for immunoprecipitation with appropriate primary antibody (anti-acetylated lysine anti-ACE-K antibodies 1:100 dilution, #9441, Cell Signaling Technology) and 5µl protein A-agarose beads (#P1406, Sigma). Binding reactions were performed for 16 h at 4 °C with gentle rotation. The beads were collected and washed three times with HEPES buffer. Bound proteins were eluted by boiling in Laemmli buffer and then subjected to SDS-PAGE and immunoblot analysis for RUNX2 (#8486, Cell Signaling Technology).

Osteogenic differentiation in 3D culture

To investigate the effect of inhibition of HDAC on the osteogenic differentiation which was applied in bone regeneration, 3D culture in PLC scaffolds was performed. The scaffold was prepared as previous described with adjustments [62, 64, 71]. PCL scaffold was fabricated with a technique involving solvent casting, polymer leaching, and salt particulate leaching. Firstly, PCL (polycaprolactone, Sigma-Aldrich, MW= 80,000 g/mol) and PEG (polyethylene glycol, Merck, Darmstadt, Germany, MW= 1000 g/mol) were dissolved in chloroform at a concentration of 28% w/v and stirred for 2 h to obtain a blended solution of the polymers (PCL: PEG= 1:1 w/w). NaCl particles were sieved to obtain particles with diameters in the range of 400–500 μm and added to the PCL solution (PCL: NaCl ratio = 1:30). The mixture was packed into Petri dishes, creating cylindrical molds that were 1.2 mm in diameter and 0.8 mm in thickness. The molds were placed in a ventilation hood overnight for solvent evaporation. The scaffolds were immersed in distilled water for 2 days to allow the PEG and salt particles to leach out (with the water being replaced in every 8 h) and air-dried for 24 h and vacuum-dried overnight prior to further use. To improve the hydrophilicity, scaffolds were immersed in 1M sodium hydroxide aqueous solution at 37°C for 1 h. The treated scaffolds were rinsed with deionized water and dried in vacuo for 48 h. For sterilization, the scaffolds were placed in 70% v/v ethanol for 15 min with gentle agitation and washed 2 times with sterilized PBS (Fig.3.1).

For 3D culture, firstly, the scaffolds were cut in pieces (4 mm in diameter and 1 mm in thickness). 1.5×10^5 hPDLs were seeded on the scaffold in 100 μl culture media for 1 h to settle down the cells in 48 well-plate. After 1 h, 200 μl culture media was added and the scaffolds were incubated at 37°C humidified atmosphere with 5%

CO_2. After 24 h, the media was replaced by osteogenic medium in the presence or absence of the HDAC inhibitor (single dose). The medium was replaced every 3 days for 14 days. Calcium deposition was investigated by Von Kossa and Alizarin red-S staining. The amount of calcium following Alizarin red-S staining was quantified by destaining with 10% cetylpyridinium chloride monohydrate (Sigma) in 10 mM sodium phosphate at room temperature for 15 min and spectrophotometically read at 570 nm.

Figure 3.1: PCL/PEG scaffold.

Cell proliferation in 3D cultures

To evaluate the effect of TSA treatment on the proliferation of hPDLs in PCL/PEG scaffold, MTT assay in 3D cultures were performed. hPDLs was incubated with or without 400 nM TSA/ml growth medium for 24h. 1.5×10^5 hPDLs were seeded onto a scaffold specimen in 100 µl growth medium and osteogenic medium for 1 h to settle

down the cells in 48 well-plate. After 1 hour, 200 µl medium was added and the scaffolds were incubated at 37°C humidified atmosphere with 5% CO_2. At the end of the culture period (3 days), the medium was replaced with MTT solution as described.

Mouse calvarial defect model

This experiment was carried out on 8-week-old male C57BL/6Mlac mice (National Laboratory Animal Centre, Mahidol University, Bangkok, Thailand). The protocol was approved by the Animal Care and Use Ethical Committee, Faculty of Medicine, Chulalongkorn University. Sixteen mice were used, which translated to a total of 32 calvarial defects for each endpoint. Randomly-selected defects were implanted with scaffold only (n=4 mice), scaffold + hPDLs (n=4) and scaffold + hPDLs + TSA (n=4). The rest of the defects were closed with no implantation (i.e., control group, n=4).

One day before implantation, hPDLs were incubated with 400 nM TSA/ml growth medium. At the day of calvarial bone graft procedure, 1×10^6 cells in 100 µl of growth medium with 400 nM TSA/ml supplement will be seeded on a scaffold for 1 h to settle down the cells in a 48 well-plate. Two circular calvarial defects (4 mm in diameter and 1 mm in thickness) were created under anesthesia by intraperitoneal injection. A general anesthetic, Nembutal® (Pentobarbital), was prepared with a phosphate buffered saline into a dilution of 1:10 and a concentration of 4 mg/kg [or 8µl of dilution/wt (g)] was used. After the anesthesia was injected into the peritoneal layer (ip.), the mice's hairs were shaved with a blade, and cleaned with alcohol and povidone iodine. Next, 0.2 ml of 1% lidocaine with 1:100 000 epinephrine was injected into the subcutaneous layer of the skull. The scalp was incised into a 1.5 cm

length to clearly show the parietal bone. A cavity of 4-mm diameter was created on both right and left side of the parietal bone using a biopsy punch (Stiefel, GSK, NC, USA) with a normal saline rinse. The procedure has to be performed gently in order to avoid dura mater injury. The bone graft was then inserted into the skull cavity and stitched up with nylon 3-0. To create the cavities on mice calvarium, some anatomical landmarks were located (Fig.3.2).

Histological analysis

At 4 and 8 weeks, the mice were sacrificed and the calvarial bones were carefully excised, cleaned, and fixed immediately with 10% buffered formalin (24 h at 4°C). After fixation, explants were rinsed with PBS, decalcified using Decalcifier II (#3800420, Leica Biosystems, Wetzlar, Germany). The specimens were dehydrated in graded ethanol solutions, xylene then embedded in paraffin, sectioned (10 µm in thickness), and stained with Hematoxylin/Eosin (H&E) for tissue structure and Masson's Trichrome including Weigert's hematoxylin for cell nuclei (black), Biebrich scarlet for cytoplasm (red), Aniline blue for collagen and bone (blue). The digital images of the sections were scanned by a visual slide microscope (Mirax desk, Carl Zeiss, Göttingen, Germany).
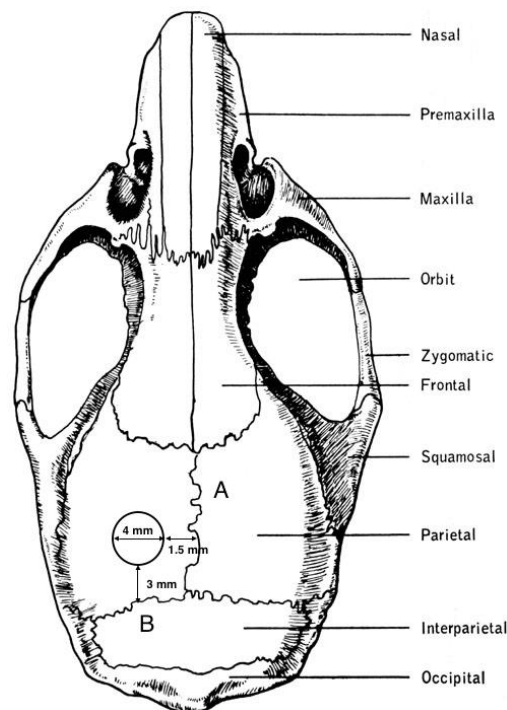
Figure 3.2: Anatomical landmarks of mouse calvarium. A cavity of 4-mm diameter created on each side of the parietal bone at 1.5 mm from the sagittal suture (A) and 3 mm from the lambdoid suture (B). Modified from http://pixshark.com/mouse-skull-anatomy.htm.

In vivo imaging with micro-CT

Micro–X-ray computed tomography (micro-CT) was performed on calvarial specimens. After being scarified, calvarial bones were carefully excised, cleaned, and fixed immediately with 10% buffered formalin (24 h at 4°C), rinsed with PBS, then stored in 70% ethanol at 4°C until scanning. Samples were typically scanned in 70% alcohol using micro-CT scanner (SCANCO Medical AG, µCT 35, Switzerland). To position the sample, a holder with a 20-mm diameter and 75-mm height was used with the reconstruction 20µm voxels (volume elements). The reference lines were

created from scout view to determine the analyzed area. The microfocus X-ray tube was operated at 70 kV, 114μA, 8W. The micro CT program was adjusted to a threshold of 241. The mineral deposition and the morphology of skull cavity were evaluated. In detail, total volume TV (mm^3), bone volume BV (mm^3) and the relative volume of calcified tissue in the selected volume of interest VOI (BV/TV) were assessed.

Immunohistochemistry assay

To confirm the presence of the human donor cells in the scaffolds, immuno-histochemistry staining was conducted with Anti-Integrin $β_1$ Mouse mAb (host: mouse, immunogen: human Integrin $β_1$, specie: human, not rat, not mouse) (#CP26, Merck Millipore). After fixing the bone specimens in mild paraformaldehyde fixed tissue (2% for 24 h at 4°C), paraffin-embedded sections were deparaffinized and rehydrated. After immersion in 1% hydrogen peroxide, the sections were blocked in BSA and incubated with primary antibody at 4°C overnight. After washing and developing with biotinylated secondary antibody (Dako Envision+ System-HRP Labelled Polymer goat anti-mouse, #K4001, Dako North America, CA, USA) Dako Liquid DAB+ Substrate Chromogen System (#K3468, Dako) was added to the section. Counterstaining with hematoxylin was carried out before slides were mounted. Staining intensity was evaluated under microscope.

ELISA analysis for immune response

To verify the inflammatory reaction and immune response *in vivo* after xenogenic transplantation, total mouse IgG was detected. After sacrificed for calvarial bone collection, the chest was opened to expose heart. 1 ml syringe with a 25-gauge needle was used to withdraw an appropriate amount of blood through the right ventricle following by transferring the blood into a new eppendorf tube. The samples were kept on ice. For serum collection, the blood was allowed to clot for 30 minutes before centrifugation for 5 minutes at 10,000 G, 4°C. The supernatant was transferred to a new eppendorf tube and stored at -80°C for further experiments. The base line of total IgG level was verified in the mice before surgery.

The mouse serum was used for the quantitative measurement of total mouse Immunoglobulin G (IgG) using an IgG mouse ELISA Kit (#KA1945, Abnova, Taipei, Taiwan). 5 μl of serum was diluted 50,000-fold in 1X Diluent Buffer. After that, 100 μl of each sample per well was added following by sealing the plate and incubating for 1 h at room temperature under plate shaker. The samples were washed four times by 1X Wash Solution and excess liquid was removed. Next, 100 μl 1X enzyme-antibody conjugate (anti- Mouse IgG antibody conjugated with horseradish peroxidase) was added to each well, which was then incubated for 30 min at room temperature. Following washing four times, 100 μl 3,3′,5,5′-Tetramethylbenzidine (TMB) chromogenic substrate solution was added to each well followed by adding 100 μL stop solution, after which the blue color development was immediately recorded using a microplate reader at 450 nm wavelength.

For detecting anti-human antigen-specific mouse IgG (hPDL-specific mouse IgG), the IgG mouse ELISA kit was used with modification to perform modified sandwich-ELISA. Firstly, the high affinity protein binding 96 well-plate (#9018, Costar Corning, New York, NY, USA) was coated with 100 μl of 10^5 hPDl lysates/well, which was collected by modified RIPA buffer (50 mM Tris-HCl, pH 7.4, 150 mM NaCl, 1% NP-40, 0.25% sodium deoxycholate, 1 mM EDTA) supplemented with protease inhibitor, and incubated overnight at 4°C. After washing the microtiter plate twice with Wash Solution, 350 μl/well and removing the liquid, 100 μl Blocking solution (1% BSA in PBS) was added for 1 hour at room temperature. Following washing, 100 μl of each mouse serum sample (1:200 dilution) per well was added and ELISA was performed. The relative optical density of IgG was measured by microplate reader at 450 nm.

To generate the positive control, the hPDL-specific mouse IgG was induced by immunization of 8-week-old male C57BL/6Mlac mice. Following by 5 continuous freezing-thaw cycles in liquid nitrogen and water bath (37°C), 10^6 hPDL lysate in 100 μl PBS was emulsified with 100 μl Freund's Complete Adjuvant, Modified, Mycobacterium butyricum CFA (#344289, Calbiochem, Merck Millipore) to produce water-in-oil emulsions of immunogens. Then the emulsion was injected i.p. to mice. After one week the mice were boosted by hPDL lysate and Freund's Adjuvant, Incomplete IFA (# F5506, Sigma). Mouse serum was collected after another one week and performed ELISA.

Data analysis

All experiments were performed three to four times. The means and standard deviations (SD) for each set of data (cell number, fold change of ALP activity, gene expression, optical density of Alizarin red staining elution, micro-CT, ELISA results) were calculated. For statistical analysis, the Shapiro–Wilk test was used to verify the normality of data. For data with non-normal distribution, Mann-Whitney U test was used to compare between groups. For data with normal distribution, independent samples comparison t-test, and one-way ANOVA with Dunnett T3 (unequal variances) or Tukey HSD post-hoc test (equal variances) were used to compare between groups using SPSS v.21 (IBM, New York, NY, USA) with the level of significance being 0.05.
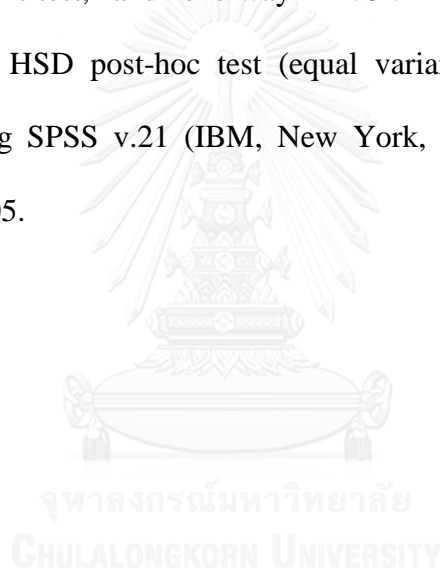
Chapter 4: Results

Effects of TSA on hPDL morphology and viability

The different concentrations of TSA up to 400 nM or its vehicle 0.4% DMSO did not result in obvious morphological changes. The higher doses appeared to induce a slightly elongated cell shape but they remained typical fibroblast-like (Fig.4.1A). However, the highest dose of TSA used, 800 nM, resulted in a greatly reduced number of cells, being 54% compared the control cultures. In order to test the effect of TSA on hPDL number and viability, the MTT assay was utilized in growth medium and osteogenic medium. In the presence of up to 400 nM TSA, no effect of the inhibitor was found after 3 days of culturing. The highest concentration used resulted in a significantly decreased read out, indicating the reduction in cell viability at that concentration (Fig.4.1B). In all subsequent experiments, the highest dose of TSA used was 400 nM.
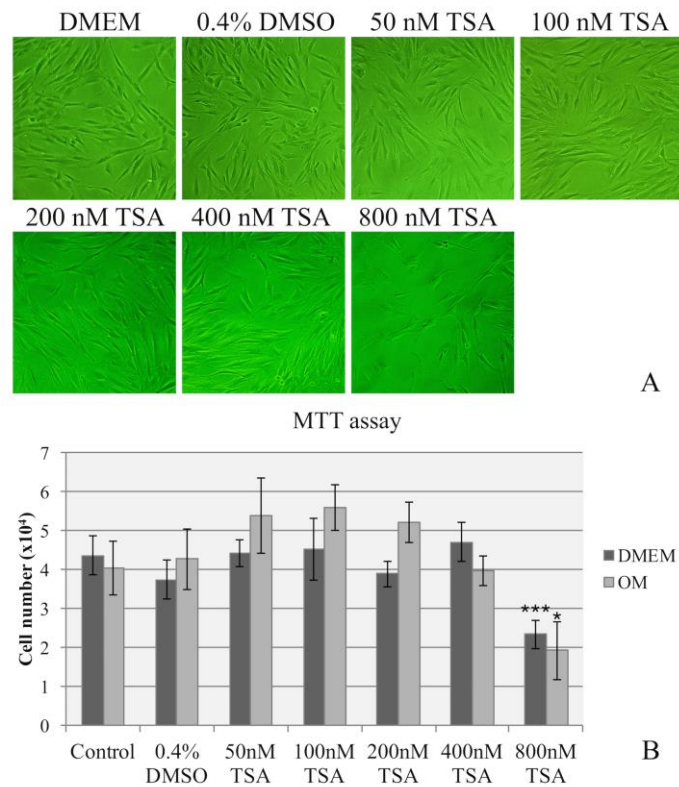
Figure 4.1: Changes of PDL cell viability and morphology following TSA incubation after 3 days. A) Morphology of hPDLs exposed to the drug. B) Cell viability of cells cultured with and without TSA in DMEM and osteogenic medium (OM) was measured by MTT assay (one-way ANOVA, Tukey HSD post-hoc test 800nM TSA groups vs. other groups, *p<0.05, **p<0.01, ***p<0.001).

Changes of osteoblast-related gene expression in TSA incubated hPDLs

To determine the possible role of the activity of HDACs on osteogenic differentiation, the inhibitor TSA was added to hPDLs in osteogenic inducing medium for 10 days. Osteoblast-specific gene expression during the course of differentiation was monitored by semi-quantitative RT-PCR (Fig.4.2). After three days in osteogenic medium, inhibition of HDACs resulted in a significantly up-regulated expression of *COL1, ALP, BSP*, and *SOST* (Fig.4.3A).

At intermediate stage of osteogenic differentiation of hPDLs (5 days), most of osteoblast-related genes were increased compared to the first stage. Notably, significant up-regulation of BSP and SOST were observed up to 2.6 and 1.7 fold, respectively (Fig.4.3B). Other intermediate to late markers of bone matrix such as *DSPP* and *OPN* were also significantly up-regulated in a time-dependent manner in the TSA group.

A similar accelerated pattern of osteogenic differentiation in hPDLs was also observed at day 10 after TSA incubation. There was a 12, 6.4, and 6.5-fold increased expression of *DMP1*, *OC* and *OPN* in TSA-incubated cells, respectively (Fig.4.3C). In addition, at this time point, *BSP* was decreased in TSA incubated group, which is a characteristic of mature osteoblasts.

While osteoblast-related markers increased significantly upon inhibition of HDACs, the osteoblast-associated transcription factors *RUNX2* and *OSX* were not altered. Up-regulation of these genes was only found to correspond with the differentiation medium in both control and TSA incubated groups in comparison with the normal condition. To confirm the changes in expression of these genes, quantitative real-time RT-PCRs were performed with selected genes related to

different stages of differentiation. Real-time RT-PCR confirmed the significant up-
and down-regulation of *ALP, COL-1, BSP, OC, OPN* at the respective time points
(Fig.4.3D). These data demonstrated that inhibition of HDAC activity during
osteogenic differentiation resulted in an acceleration of osteoblast-related gene
expression and therefore enhance the differentiation process of hPDL into an
osteogenic lineage.
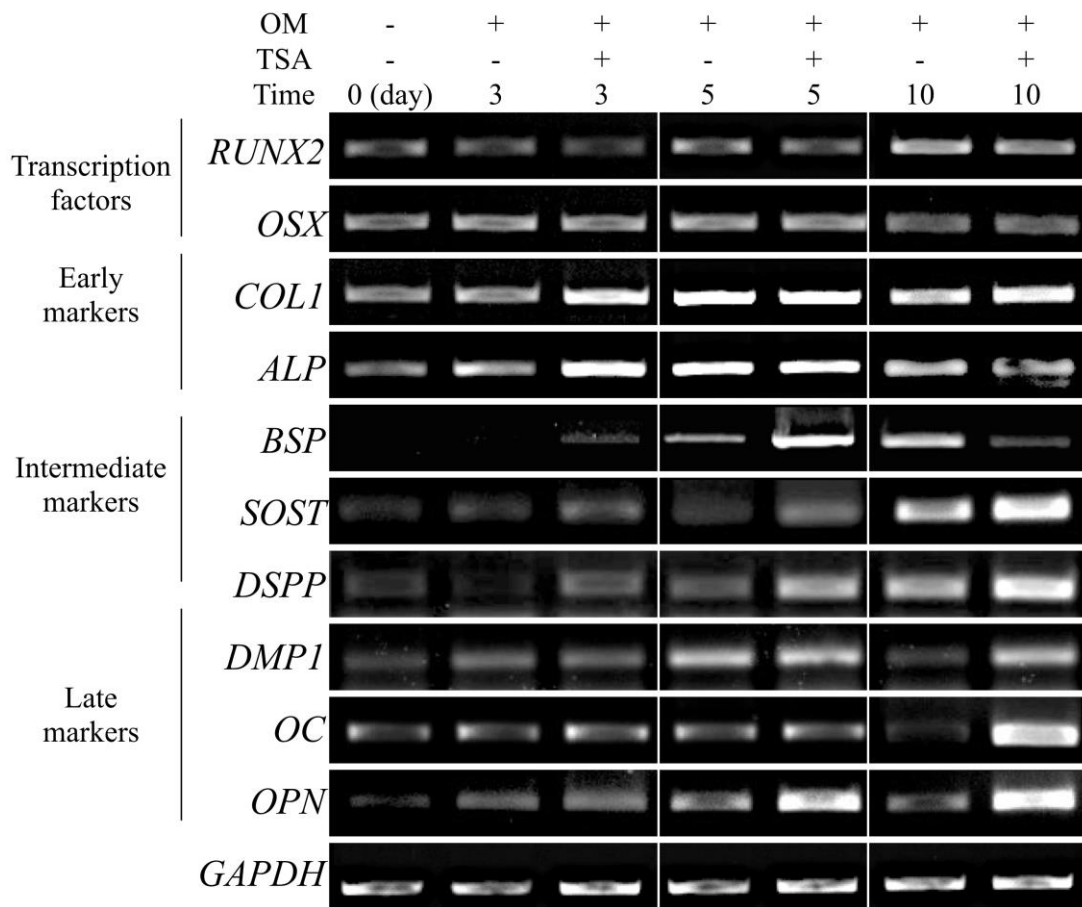
Figure 4.2: Effect of 400nM TSA on expression of bone related genes during osteogenesis of hPDLs by RT-PCR. TSA shifted the expression of early, intermediate and late bone associated markers. OM: osteogenic medium.
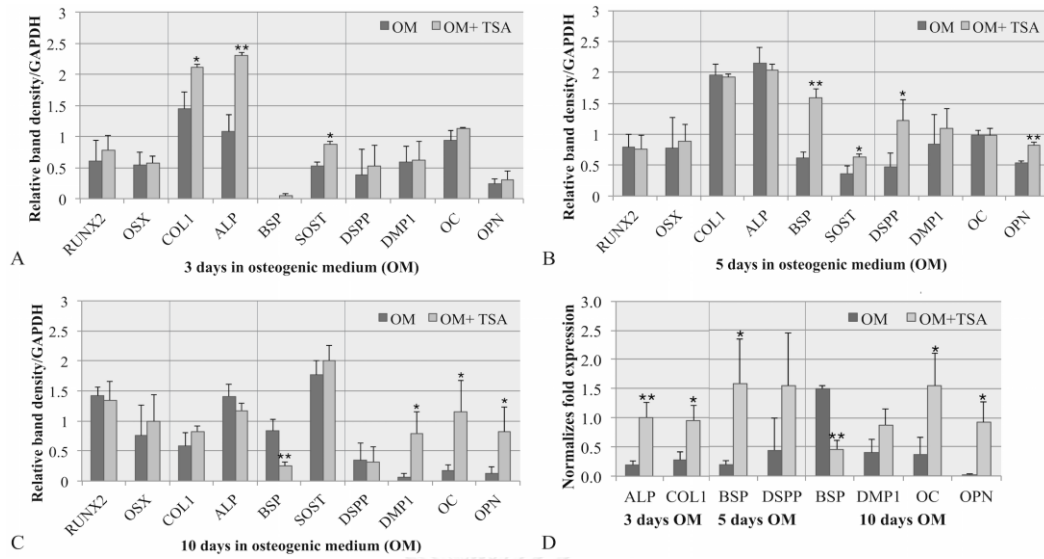
Figure 4.3: Expression of bone related gene expression during the onset of osteogenesis in hPDLs cultured with and without TSA. A-C: Semi-quantitative RT-PCR of relative expression/GAPDH of osteoblast-related genes at 3, 5 and 10 days. D: Effect of TSA on osteoblast-related gene expression was confirmed by quantitive real-time RT-PCR (independent samples t-test between control and TSA incubated group, *p<0.05, **p<0.01. OM: osteogenic medium).

TSA enhanced the osteogenesis but not adipogenesis of hPDLs

To analyze the effect of TSA on osteogenic differentiation in the actual function of these cells, we performed ALP activity assays and assessed bone nodule formation. At early and intermediate stage (3 and 5 days), inhibition of HDACs resulted in an increased ALP activity (Fig.4.4). The inhibitor used at 400nM induced the highest ALP activity while 100nM did not show a significant increase. After 10 days, ALP activity was much stronger increased in all groups compared to the earlier time points. There was a trend in reduction of ALP activity in TSA dose-dependent way at this time point.

Mineral deposition was evaluated using Von Kossa and Alizarin red staining. Inhibition of HDAC activity enhanced mineral deposition. This effect proved to be inhibitor dose-dependent (Fig.4.5). Microscopic examination clearly demonstrated the increase in number of mineralized nodules in all TSA incubated groups.

To clarify whether the effect of the inhibitor was specific for osteogenenic differentiation, we used adipogenic medium with or without the HDAC inhibitor. Two main markers of adipogenic differentiation, *LPL* and *PPARγ2*, were decreased in the TSA incubated group compared to the control groups (Fig.4.6A). When cultured in adipogenic medium, hPDLs were able to differentiate in to Oil red O positive adipocyte-like cells as demonstrated in Fig.4.6B. However, treatment with TSA was failed to driven hPDLs toward adipogenic fate (Fig.4.6B).

ALP activity (Unit/µg protein)
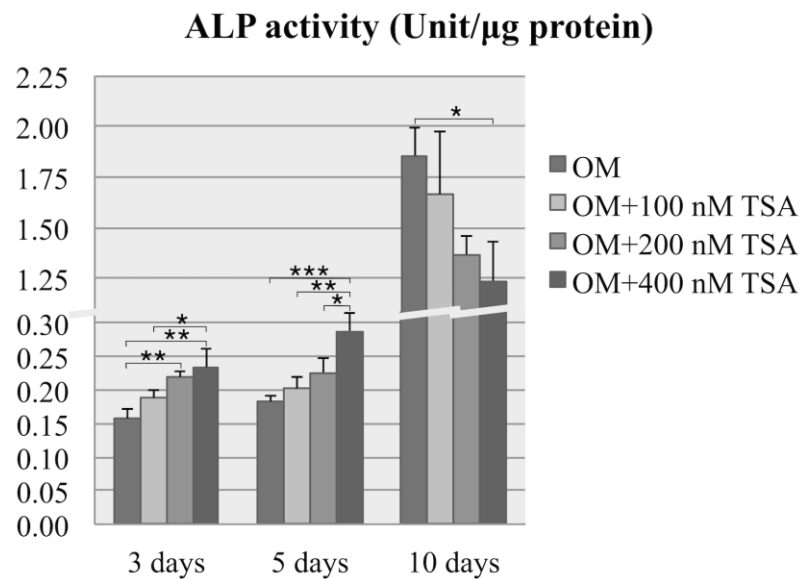
Figure 4.4: Effect of TSA on the production of alkaline phosphatase enzyme during the onset of osteogenesis analyzed by ALP activity assay. TSA enhanced the production of alkaline phosphatase in a dose-dependent manner at 3 and 5 days while there was a trend in reduction of ALP activity in 10 days. (one-way ANOVA, Tukey HSD post-hoc test, *$p<0.05$, **$p<0.01$, ***$p<0.001$).
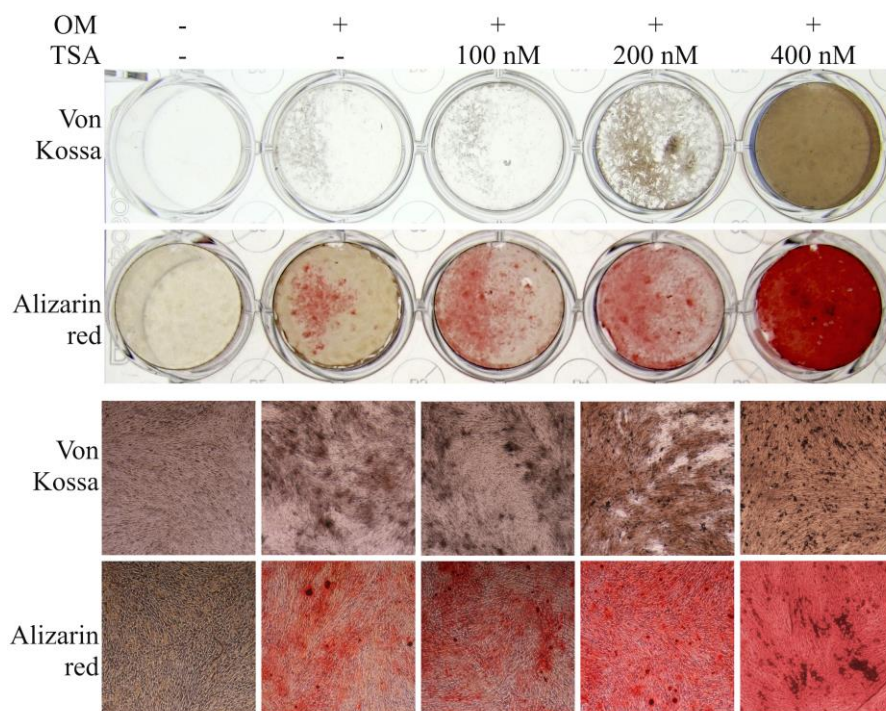
Figure 4.5: TSA enhanced, in a dose-dependent manner, mineral deposition of hPDLs after 10 days in osteogenic medium (OM) observed by Von Kossa and Alizarin red staining. Microscopic images of mineralized nodule formation. (lower panel: x40).
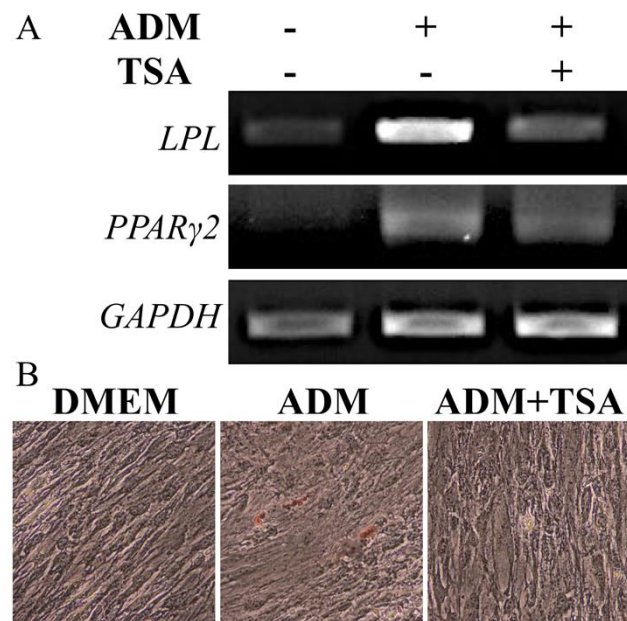
Figure 4.6: TSA inhibited the adipogenic differentiation of hPDLs. A) Adipocyte-related gene expression examined by semi-quantitative RT-PCR. TSA (400nM) did not alter adipocyte-related gene expression during adipogenic induction for 7 days in ADM (Adipogenic medium). B) Oil red O staining in growth medium (DMEM), ADM and ADM+ TSA after 21 days of differentiation (200x).

Osteogenic differentiation and TSA promoted RUNX2 protein expression and the hyperacetylation on histone H3 in hPDLs

To evaluate the effect of HDAC inhibitor on alteration of histone acetylation during osteogenic differentiation in hPDLs, RUNX2 protein expression and acetylated histone H3 at lysines K9/K14 were verified by immunoblotting. Runx2 protein was increased during the course of osteogenic differentiation, especially in inhibitor treated group (Fig.4.7A). Concomitantly, level of acetylated histone H3 was gradually increased while total histone H3 was used as control. (Fig.4.7B). Immunoprecipitation also indicated that TSA induced acetylated RUNX2 in both growth and osteogenic media for 2days. The levels of acetylated RUNX2 in ostegenic media were higher than in normal condition. Inhibition of HDAC activity induced Runx2 production and acetylation, and hyperacetylation of histone H3.
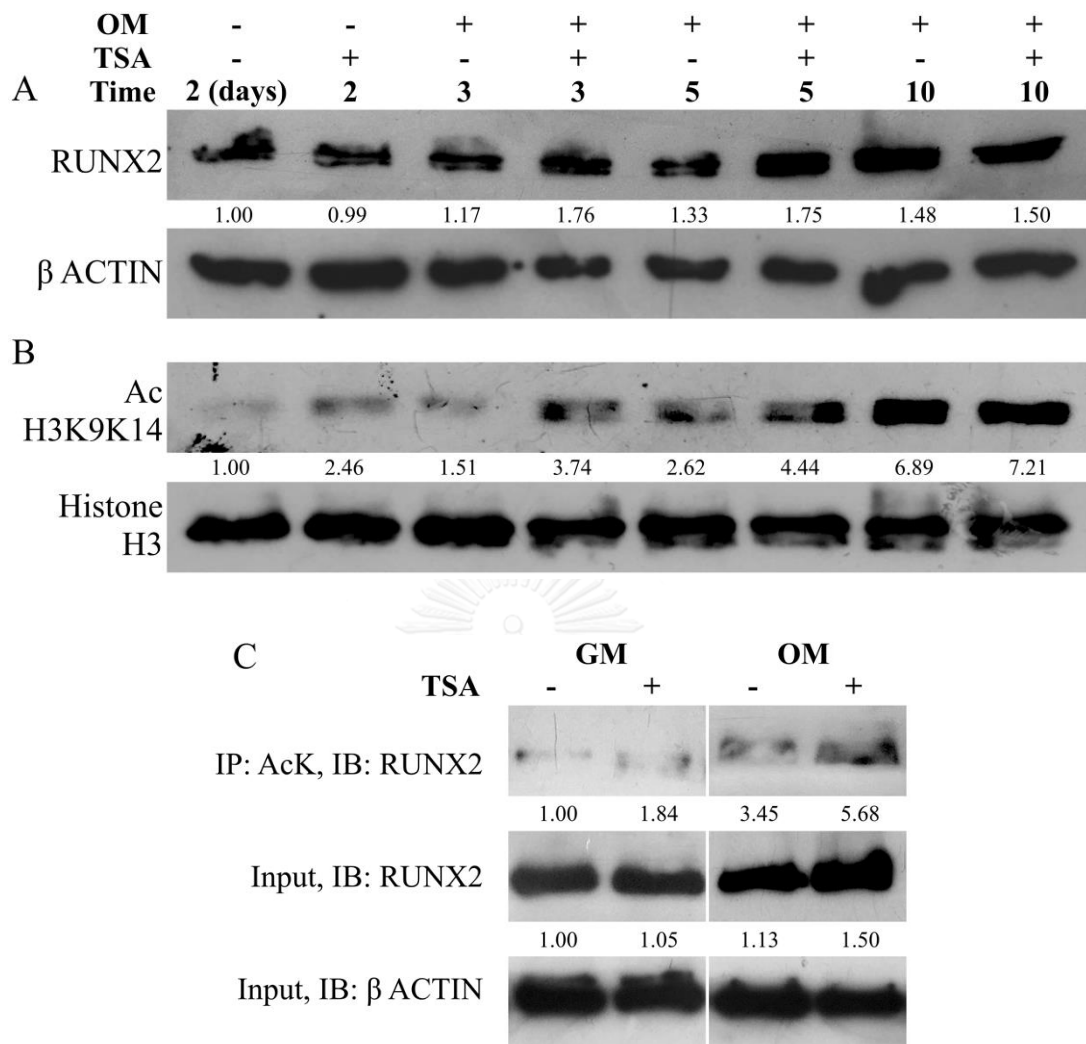
Figure 4.7: Effect of TSA (400nM) on Runx2 and Ac H3K9K14 protein expression.

A) TSA enhanced the Runx2 protein production during osteogenic differentiation. B)

Acetylation of histone H3 was up-regulated during osteogenic differentiation in a time

dependent manner and HDAC inhibitor (400nM TSA) enhanced this process. C) TSA

induced acetyalated Runx2 by immunoprecipitation (IP). IB: Immunoblotting; AcK:

Actylated lysine; H3K9K14: acetyl histone H3 lysine K9/K14; H3: total histone H3.

Osteogenic differentiation and TSA altered the production of HDACs in hPDLs

In an attempt to elucidate the mechanisms involved in HDAC-induced cell differentiation, we examined the protein expression of HDACs in class I (HDAC 1, 2, 3), class IIa (HDAC 4) and class IIb (HDAC 6). Western blot analysis of whole cell extracts showed that hPDLs expressed all involved HDAC 1, 2, 3, 4 and HDAC 6 (Fig.4.8A). Interestingly, the expression of HDAC 3 was found to decrease during the onset of osteoblastic differentiation while HDAC 2 tended to decrease from proliferation to differentiation. During the time course of osteogenic induction, the expression of HDAC 1 and HDAC 3 (class I) were decreased in the inhibitor incubated group. HDAC3 expression level was totally abolished at day 10 in hPDLs incubated with TSA. Slightly decreased of HDAC 4 (class IIa) and HDAC 6 (class IIb) was observed at day 10 in TSA incubated group. This data strongly suggests the involvement of HDAC3 in osteogenic differentiation.

The level of HDAC 3 was not significantly altered when hPDLs were cultured in control media for 5-10 days. Incubation with TSA slightly decreased HDAC 3 protein when cultured for 10 days in control media. This data indicated that regardless of induction of osteogenesis, TSA has a direct effect on HDAC 3 protein level (Fig.4.8B).
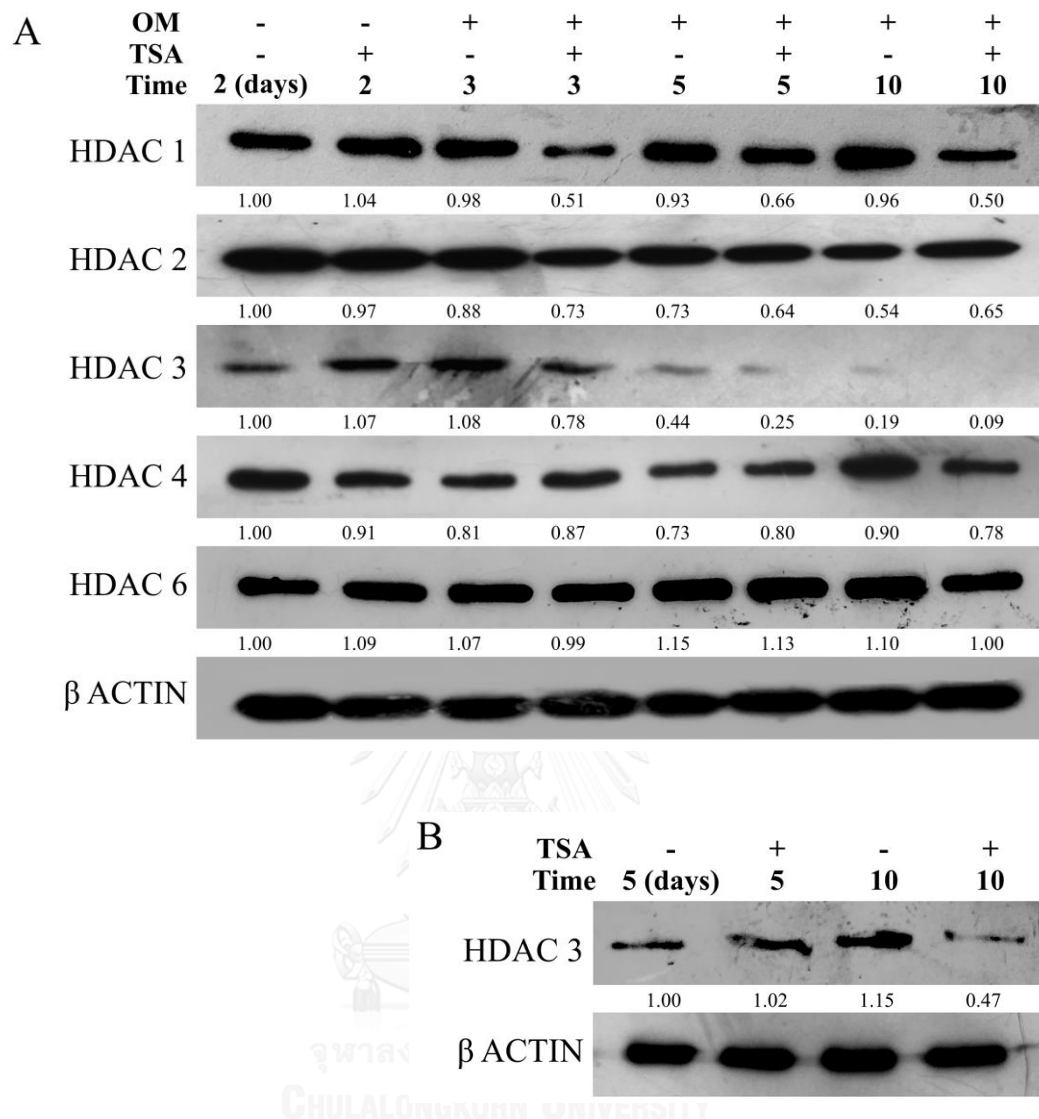
Figure 4.8: Effect of TSA (400nM) on HDACs protein expression. A) TSA gradually down-regulated the expression of HDAC 1 and HDAC 3 during the onset of osteogenesis. The endogenous expression of HDAC 3 was also affected by osteogenic induction. B) Level of HDAC 3 after hPDLs were cultured in growth medium for 5 and 10 days with or without TSA. Fold change number of protein band density was presented below each band.

TSA enhanced mineralization of hPDLs in 3D culture model

HDAC inhibitor enhanced the mineral deposition of hPDLs in PCL/PEG scaffold after 14 days in osteogenic medium. The quantitated amount of calcium following Alizarin red-S staining demonstrated significant difference in TSA-pretreatment in comparison with growth medium and osteogenic medium groups (Fig.4.9A, B). Moreover, TSA-pretreatment did not alter cell proliferation and attachment for 3 days in scaffold as determined by MTT assay (Fig.4.9C).
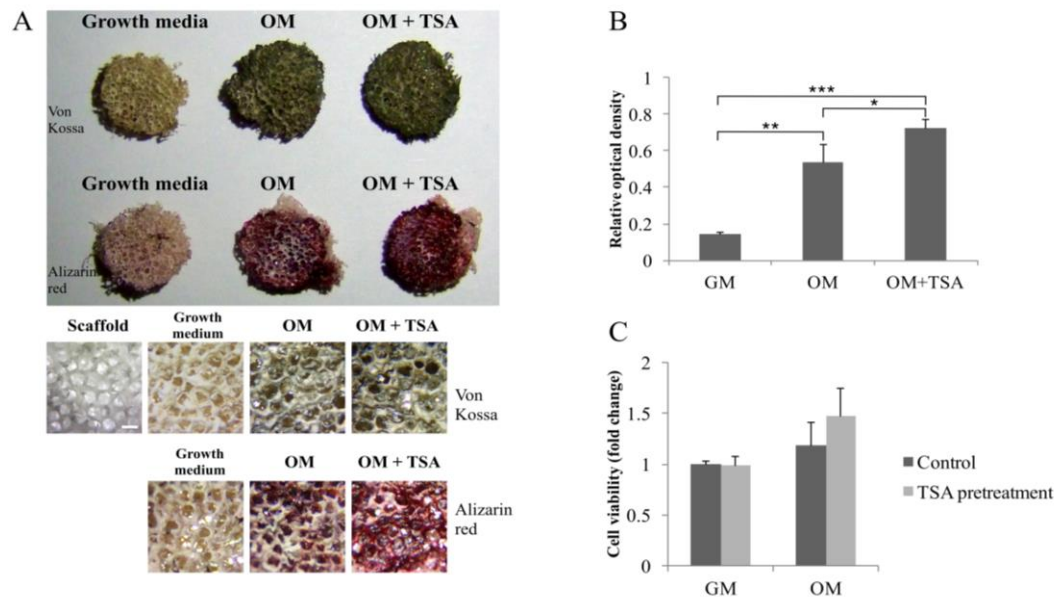
Figure 4.9: Effect of TSA on hPDLs in in PCL/PEG scaffold. A) TSA enhanced the mineral deposition after 14 days by Von Kossa and Alizarin red staining, scale bar 500 μm. B) Quantification of mineral deposition by Alizarin red elution of hPDLs with and without TSA. C) Effect of TSA pretreatment (for 24h) on hPDLs proliferation and attachment for 3 days evaluated by MTT assay. (GM: growth media, OM: osteogenic media; one-way ANOVA, Turkey HSD post hoc test, * $p < 0.05$, ** $p < 0.01$, *** $p < 0.001$).

TSA enhanced bone regeneration of hPDLs *in vivo*

TSA promoted bone regeneration in mouse calvarial defect model at 4 and 8 weeks when observed by micro-CT scanning and histological analysis. Fig.4.10A, B showed the anatomical location of defect and H&E staining of the specimens. Masson's Trichrome stain demonstrated the increase in collagen and mineralized matrix in TSA-pretreatment group at both 4 and 8 weeks after implantation (Fig.4.10C, D). It should be note that, newly formed bone present in the middle of defects instead of the periphery. The results were more magnificent after 8 weeks. Meanwhile, there was no healing in defect without scaffolds at any time points (Fig.4.11A). Quantification of bone volume/total volume (BV/TV) from micro-CT scanning showed the significant difference in scaffold-hPDL-TSA groups comparing with the other two groups after 4 and 8 weeks (Fig.4.11B).
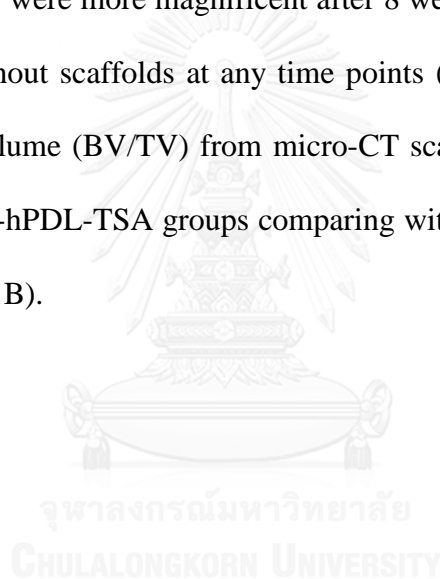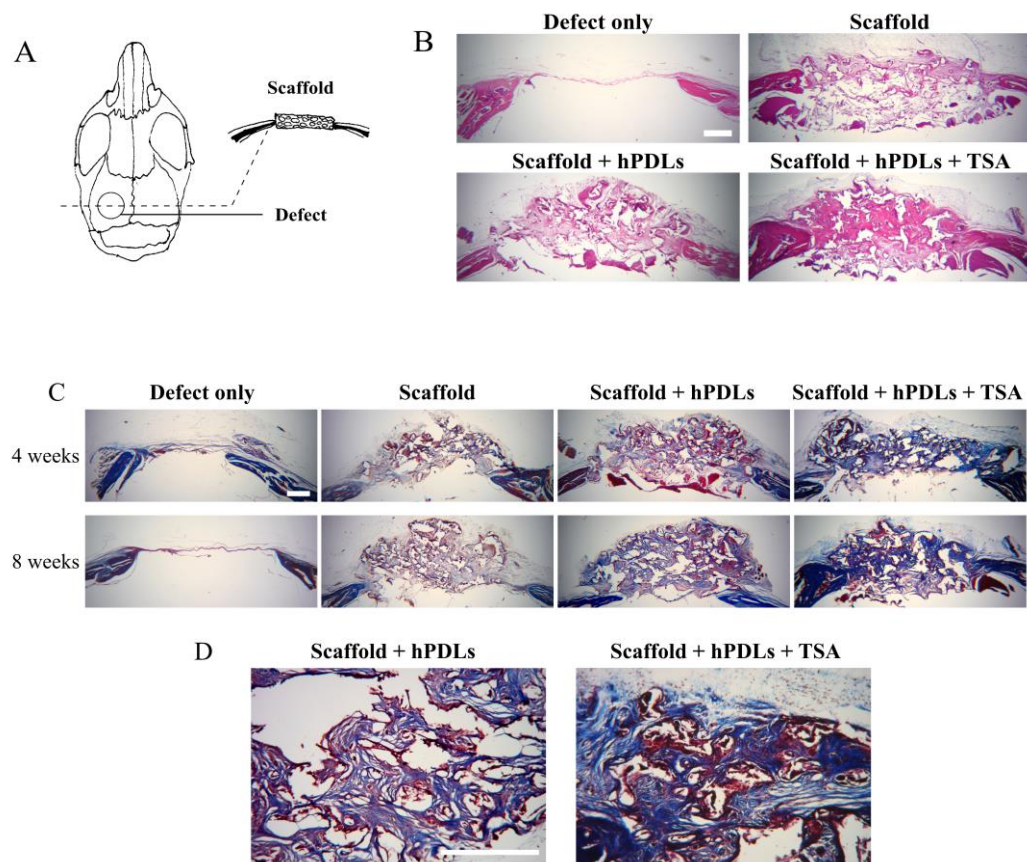
Figure 4.10: Effect of TSA on bone regeneration in mouse calvarial defect model A).
B) H&E staining showed the microscopic structure of tissue at 8 weeks. C) Masson's
Trichrome staining of mice calvaria defects at 4, 8 weeks. D) High magnification of
scaffold + hPDLs groups with and without TSA at 8 weeks (scale bar 500 μm).
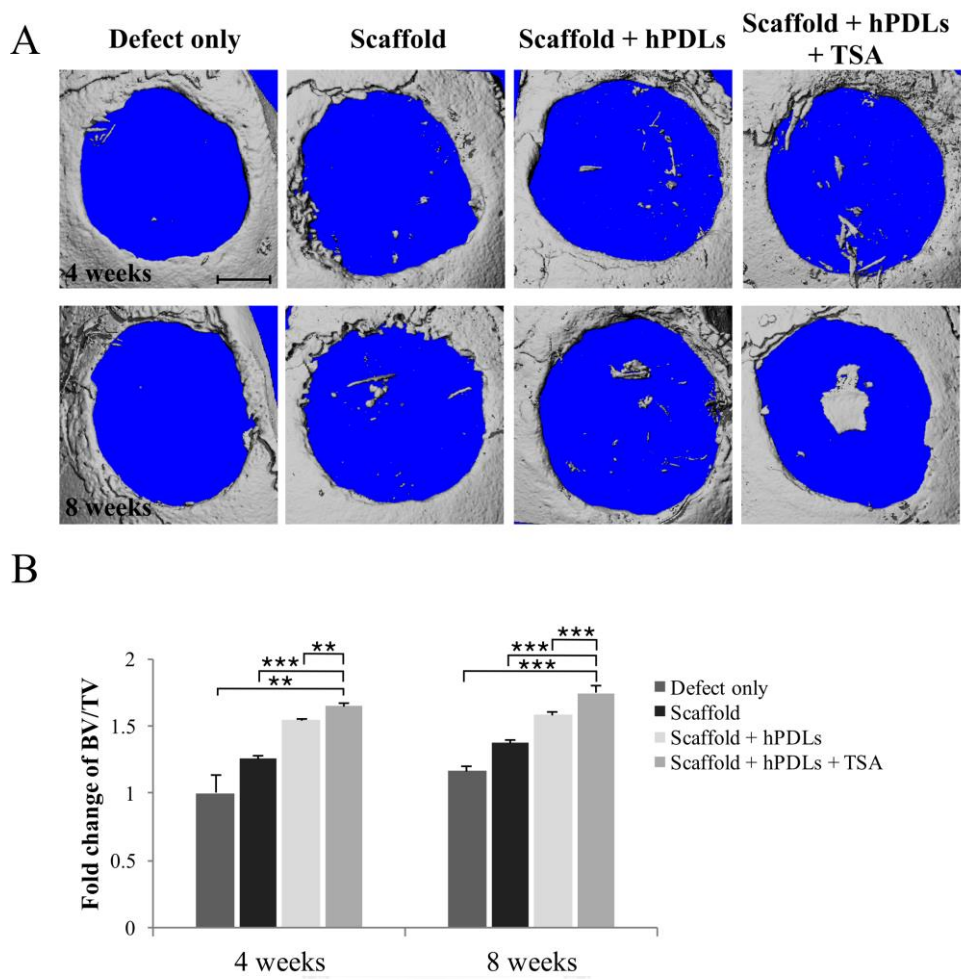
Figure 4.11: Effect of TSA on bone regeneration in mouse calvarial defect model by micro-CT scanning for 4 and 8 weeks. A) New bone formation in mouse calvarial defect. B) Quantification of bone volume in total volume (BV/TV). Scale bar: 1000 μm; one-way ANOVA, Dunnett T3 (4 weeks), Turkey HSD post hoc test (8 weeks), * p< 0.05, ** p< 0.01, *** p< 0.001.

Mouse calvarial defect model did not affect the survival of hPDLs

To verify the existence and survival of hPDLs after transplanting into mouse calvarial defect as xenografts, immunohistochemistry against Human Integrin β_1 was performed. Human Integrin β_1 was detected only in groups with hPDLs (with and without TSA). The expression was not detected in defect with scaffold only (Fig.4.12).
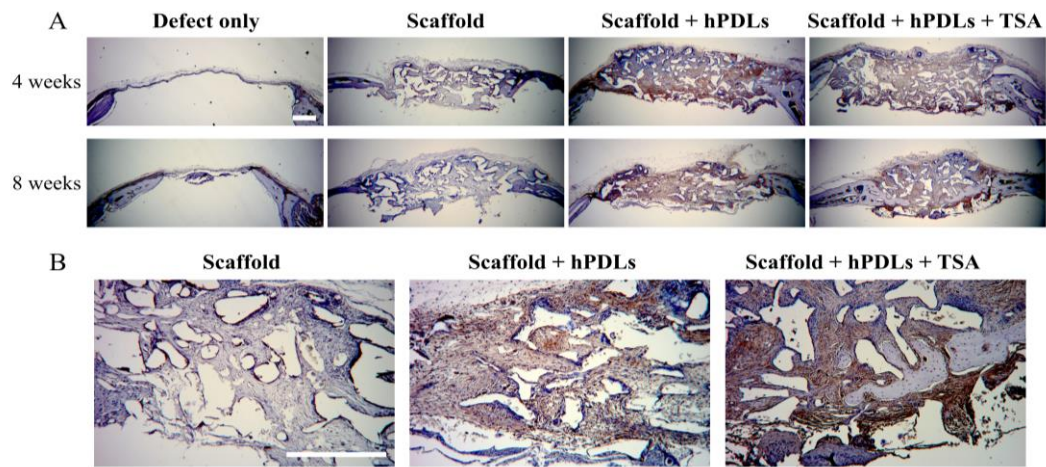
Figure 4.12: The expression human Integrin β_1 in hPDLs in in mouse calvarial defect model by immunohistochemistry. A). Immunohistochemistry stain of the calvaria defects at 4, 8 weeks. B) High magnification of scaffold, with and without hPDLs, TSA at 8 weeks. Scale bar: 500 μm.

hPDLs did not stimulated significant immune response in mice

To verify whether hPDLs trigger unforeseen immunological response after transplanting into mouse calvarial defect as a xenograft, total mouse IgG and hPDLs-specific mouse IgG were measured. There was a significant up-regulation of total IgG in surgery groups in comparison with baseline, especially at 4 weeks after operation (Fig.20A). However, there was no significant difference in total IgG in all surgical groups regardless of any treatments. hPDLs-specific mouse IgG level in immunized positive control group was significantly higher than other groups (Fig.20B). Although there was a slightly up-regulation of hPDLs-specific mouse IgG level in defect containing hPDLs, the difference was not significant.
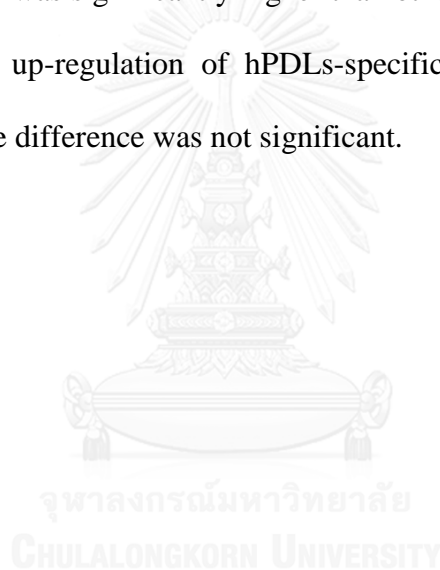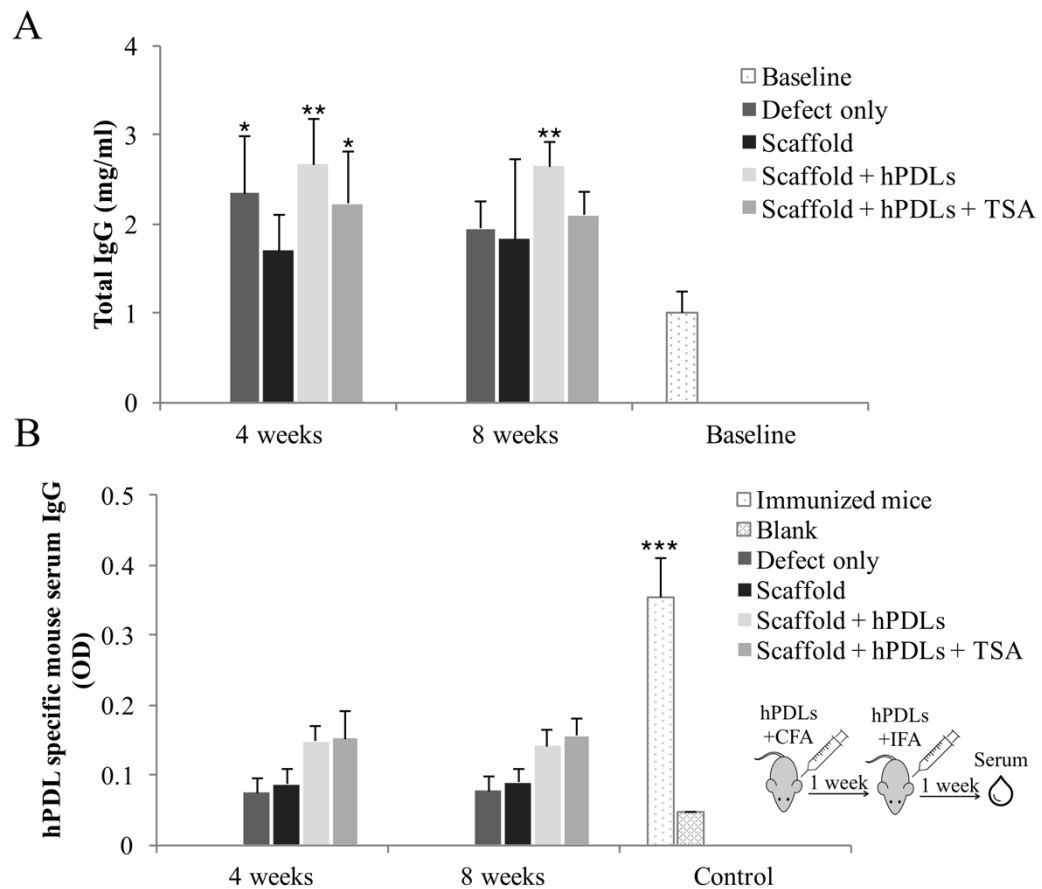
Figure 4.13: Effect of hPDLs on mouse total IgG and hPDLs-specific IgG. A) Level of total IgG in mouse serum by ELISA. B) Level of hPDLs-specific mouse -specific mouse IgG (one-way ANOVA, Turkey HSD post hoc test experiment groups vs. baseline (A), vs. immunized mice (B), n=4).

Chapter 5: Discussion

In the present study, we demonstrate for the first time that inhibition of the activity of HDACs with the pan HDAC inhibitor TSA enhances osteogenic but not adipogenic differentiation of hPDLs. While HATs transfer the acetyl groups to the side chain of lysine residues at the N-terminal tail of histones, HDACs deacetylate lysine residues and counterbalance the activity of HATs. They also catalyze non-histone proteins which leads to chromatin remodeling and limit the binding of transcription factors at target gene promoters. Several HDACs have been identified as regulators of osteoblastic differentiation and maturation. For instance, HDAC 1, 3, 7, 8 suppress osteogenic differentiation of bone marrow stromal cells and osteoblasts [50, 51, 73, 74]. Using HDAC inhibitors such as valproic acid (VPA), TSA, sodium butyrate (NaB) acceleration was shown of osteogenic differentiation by human adipose tissue-derived stromal cells, bone marrow stromal cells, and MC3T3-E1 cells [9, 10].

Bone marrow cells, dental pulp cells, as well as hPDLs have a strong potential to differentiate into osteoblasts. Previous studies showed that NaB and VPA can up regulate the gene expression of *OC, OPN* and *BSP* in hPDL and dental pulp stem cells [52, 75]. Inhibition of HDAC activity appears to boost the onset of osteogenesis in these cells from the early stage of differentiation. During this early phase the expression of the genes *COL1* and *ALP* were up-regulated, *BSP* and other genes were up-regulated during the intermediate phase and *OC* and *OPN* during the later stage of differentiation. We also found a slight up-regulation of *SOST*, suggesting an osteogenic maturation of hPDLs. Gregoire et al. found that HDAC 3 suppressed the Myocyte Enhancer Factor 2 (MEF2) [76]; this factor binds to a distant downstream

SOST gene enhancer and modulates SOST expression [77]. However, the role of HDAC enzymes in SOST expression is still not clear which are the different effects between class I and II HDAC on SOST gene regulation in osteocytic cells [78]. The observed up-regulation of several genes was confirmed by the corresponding cellular functional assays like ALP activity and bone nodule formation assay. ALP activities in the experimental groups were found to be highest during the first stage (3 days) of osteoblastic differentiation in hPDLs. This effect was still maintained at the day 5 time point. *ALP* is among the first functional genes expressed in the process of calcification and plays an essential role in the formation of mineral crystallites during bone formation [79]. *BSP* which is a marker of middle stage was also expressed higher in the TSA incubated group starting from three days of differentiation, was highest expressed at the 5 day stage and declined thereafter. In the later stages, the noncollagenous extracellular matrix proteins such as osteocalcin and osteopontin, which are responsible for bone matrix deposition and maturation, were up-regulated significantly. Interestingly, during the later stage of osteogenic differentiation, TSA incubation tended to decrease ALP activity in a dose-dependent manner. This finding appears to coincide with the notion that *ALP* is expressed early in development and significantly reduces at later stages of osteoblastic differentiation. This expression is opposite to the regulation of expression of osteocalcin [80]. The efficiency of TSA to induce osteogenic differentiation in hPDLs was clearly demonstrated by bone nodule formation assay using both Von Kossa and Alizarin red staining. Alizarin red was used to identify calcium accumulation whereas Von Kossa is specific for calcium salts such as carbonate and phosphate. Using both methods we confirmed the presence of mineral deposits during the osteogenic maturation.

In our study, hPDLs were cultured and characterized as described in our previous study [69]. Data showed that the cells expressed surface markers resembling those of mesenchymal stem cells (including *NANOG, OCT-4, CD44, CD105*). By the outgrowth method from PDL tissue, the cells are pool of MSCs and fibroblasts [81]. Mesenchymal stem cells can differentiate into adipocytes. Also hPDLs were shown to have this capacity [82]. Therefore, we tested whether inhibition of HDACs could also induce adipogenic differentiation by hPDLs. No such an effect was found and therefore we conclude that in hPDLs HDACs play an important role in osteogenic but not in adipogenic differentiation. The finding suggested that TSA was not able to direct the adipogenic potential in these cells which corresponds with the previous reports about effect of HDAC inhibitors on adipogenesis [60, 83].

To evaluate the function of HDAC inhibitor in hPDLs as well as the importance of histone acetylation during osteogenic differentiation, total histone H3 and acetylated histone H3 were assessed. Several studies have shown that during normal osteoblastic differentiation, hyperacetylation of histones was noted at the osteocalcin gene promoter and the acetylation was stronger under HDAC inhibitor treatment [46, 48, 84]. Here we demonstrated the similar result on hPDLs. Our data clearly showed the increase of histone H3 acetylation at lysines K9/K14 during osteogenic differentiation while inhibition of HDAC activity even enhanced this process. Histone H3 acetylation at lysines K9/K14 play a pivotal role in epigenetic mechanisms such as being epigenetic marker representing active chromatin, defining distinct chromatin regions permissive transcriptionally for transgene expression. A permissive chromatin region is enriched in H3 acetylation [20, 85]. The predominant

in acetylation of histone H3 by inhibition of HDAC activity in hPDLs might indirectly demonstrate the increase in transcriptional accessibility of its chromatin.

In our present study, we clearly demonstrated the endogenous expression of class I (HDAC 1, 2, 3) and class II (HDAC 4, 6) HDAC proteins in hPDLs. Despite ubiquitous expression of class I HDAC in many cell types, the expression pattern of class II HDAC is cell type-restricted. Interestingly, previous studies showed that HDAC 4 was expressed in chrondocytes and marrow stem cells but not by an osteoblast cell line and HDAC 6 was not expressed or expressed weakly in some osteoblast cell lines [31, 47, 48]. We know how that hPDLs express a high level of both HDAC 4 and HDAC 6 proteins. The finding suggests a role for HDAC 4 and HDAC 6 in the functioning of hPDLs and may provide clues as by which HPDLs can be distinguished from other osteoblast-like cell types. HDAC 4 was reported to regulate chondrocyte hypertrophy and endochondral bone formation while HDAC 6 represses the p21 promoter in the immortal fibroblast-like cell line [31, 47]. Further studies need to explore the function of these enzymes in PDL cell.

TSA is reported to inhibit the activity of all class I and II HDACs [13]. The inhibition of the enzymatic activity is now shown to affect the expression of HDACs themselves. TSA induced a time-dependent decrease of HDAC 1, 2 and 3 expression during the onset of osteogenesis in hPDLs. This finding was related with previously reported function of HDAC 1 as transcriptional co-repressors of osteoblastic differentiation by interact with bone related transcription factor, RUNX2, to modulate its downstream genes like osteocalcin [50]. HDAC 1, 2 and 8 have been reported to down-regulate osteogenenic differentiation by osteoblast, bone marrow stem cells and dental pulp cells [50-52]. The expression of HDAC 3, however, was not altered in

these cell type. Knockdown of HDAC1 by the short interference RNA system stimulated osteoblast differentiation in ROS17/2.8 cells, while HDAC2 silencing produced a similar effect to that of HDAC inhibitor treatment on the expression of osteoblast- related markers in Sao-2 cells [50, 52]. HDAC1/2 establish and stabilize with mSin3A as a global transcriptional co-repressor complex. It interacts with other proteins and transcription factors including Runx2 to regulate gene expression. However, mSin3A binding domain on Runx2 has not been identified yet [86, 87]. Our results showed the same trend in reduction of HDAC1 and 2 under inhibitor treatment and during osteogenic differentiation. In this study, we demonstrated, for the first time, a decreased expression of HDAC3 during osteogenic differentiation of hPDLs. This finding strongly suggests a role for this enzyme in the modulation of osteogenic differentiation by hPDLs. In line with our finding is a study by Schroeder TM et al., who demonstrated that knocking down HDAC 3 *in vitro* by shRNA increased RUNX2 activity and the osteocalcin promoter and therefore enhanced osteogenic differentiation by osteoblasts [49]. Several studies showed that HDAC 3 can bind to RUNX2, nuclear factor of activated T cells (NFATc1), T-cell factor (TCF) and zinc finger protein 521 (Zfp521). This binding seems to suppress osteoblast-related gene expression and to regulate osteoblastic differentiation [49, 74, 88]. In our study, despite the accelerative onset of osteogenesis of hPDLs, mRNA level of RUNX2 was not altered. Though, Runx2 protein was increased during osteogenesis, slightly upregulation was observed under TSA treatment at day 3 and 5. Other HDAC inhibitor s such as NBu, VPA also increased Runx2 protein [51, 75]. Moreover, HDACs also catalyzes deacethylation process of non-histone proteins which may include transcription factors those driven bone formation. Posttranslational

modifications, such as acetylation, of these transcription factors can alter their transcriptional activity and stability. In our study, in hPDLs, acetylated Runx2 was increased under TSA treatment. It was reported previously that BMP-2 increases p300-mediated Runx2 acetylation but not Osx, enhancing the stability and transcriptional activation of Runx2 in Runx2-transfected mouse myoblast C2C12 and HEK 293 cells [89]. Infact, Runx2 has 10 lysine residues that are potential sites of ubiquitination and acetylation. When a signal comes that aims to induce RUNX activity, for example TGF-β or BMP, RUNX acetylation is increased by relatively high levels of acetyl transferase activity and ubiquitination is inhibited. This activates RUNX and protects it from proteasome-mediated degradation [90, 91]. Moreover, HDAC inhibitors such as TSA, CHAP27, SCOP402 also stimulated Runx2 acetylation and protein in HEK 293 cells [89]. Our finding coupled the fact that HDAC inhibitors increase the level of the Runx2 protein and acetylated Runx2 as well as alter the expression of HDAC3, a post translational modificator of RUNX2. Moreover, the HDAC3 protein expression levels were significantly down-regulated following incubation with HDAC inhibitors, suggesting that the expression of HDAC3 itself is regulated by histone deacetylation [28, 92]. This correlates with our finding that under control conditions in which the level of HDAC3 was affected by inhibitor only. Up to 10 days of incubation, a slightly decrease in drug incubated group was observed indicating the effect of HDAC inhibitor in HDAC 3 level. However, it was not abolished as under the differentiation. Further study need to clarify the role of HDAC 3 in osteoblastic differentiation of hPDLs.

In our study, we verified the effect of TSA on bone regeneration by 3D culture model with PCL/PEG scaffold. The scaffold was developed and modfified from our

previous studies with PCL porous scaffold [62, 64]. 3D PCL scaffolds with highly porous and interconnected networks which implement sodium chloride and PEG as porogens gave the high potential for bone tissue engineering and no harm to MC3T3-E1 cells as well as highest mineral deposition values [64]. The incorporation of hydrophilic PEG into hydrophobic PCL enhanced the overall hydro- philicity and cell culture performance of PCL/PEG copolymer [93]. The cell growth, gene expression, and osteogenic differentiation in three types of mesenchymal stem cells, including bone marrow-derived mesenchymal stem cells (BMSCs), dental pulp stem cells (DPSCs), and adiposed-derived mesenchymal stem cells (ADSCs) in PCL scaffold was confirmed [94]. Moreover, we did not use hydroxyapatite (HA) in the scaffold to eliminate the background of mineral staining due to HA itself also stained by alizarin red [62, 64, 71]. Our results showed that pre-treatment of single dose of TSA enhanced the mineral deposition while there was difference on cell attachment and proliferation between groups indicating that TSA affected the differentiation of PDLs in long-term.

There were few studies those investigate the role of HDAC inhibitor in osteogenesis by 3D culture. Paint et al. investigated the response of DPSCs to VPA in an environment that more closely mimicked 3D bone tissue [52]. In the samples pre-treated with VPA, collagen and calcium deposits were much more intense and diffuse. Schroeder and Westendorf showed that HDAC inhibitors including TSA promoted osteoblast maturation in calvarial tissues by increasing ALP activity *ex vivo* [9]. In this study, calvaria were dissected and divided along the sagittal suture. One-half of each calvarium was cultured in vehicle and the other one-half was incubated with the indicated inhibitor. There are some studies investigating the role of HDAC inhibitor

in bone formation *in vivo.* For instant, intraperitonial injection of vorinostat into C57BL mice increased serum osteocalcin levels and osteoblast numbers in endocordical and trabecular bone surfaces [48]. Jin et al. demonstrated by using murine experiment to supported that TSA affected odontoblast differentiation and dentin formation [95]. The thicker dentin, more odontoblasts, and higher DSP detection in TSA group strongly suggested that the injected TSA may influence DPSCs, promoting odontoblast differentiation and dentin formation *in vivo.*

Up to now, there is no study investigating the application of HDAC inhibitor in bone regeneration by calvarial defect model *in vivo.* Our study, for the first time, showed that HDAC inhibitor can promote bone regeneration by mouse calvarial defect model *in vivo*. In our study, critical-sized (4mm) mouse calvarial defects were created showing that TSA enhanced new collagen and bone formation after 4 and especially at 8 weeks of scaffold grafting by hPDLs. The scaffold degradation was also observed by histological analysis. There were several studies assessing the feasibility of the use of human mesenchymal cells for tissue engineering and demonstrate that they are suitable for bone reconstruction in xenotransplantation models. Zong et al. evaluated the reconstruction effects of hMSCs and osteoblast-like cells differentiated from hMSCs in poly-lactic-co-glycolic acid (PLGA) scaffolds on the calvarial defect of rats which showed the similar regeneration effect when examined by Masson's Trichrome stainning after 10 weeks [96]. The scaffold only did not support collagen and bone regeneration as previous study in HA free PCL [71]. The results were also confirmed by micro-CT showing the significant difference in bone volume/ total volume in TSA-pretreatment group. Micro-CT allows the qualitative and quantitative assessment of the spatial and temporal mineralization of

bone formation. The availability of 3D analysis techniques, coupled to specific image processing methods, opens up new possibilities for the analysis of bone structure [65]. However, our rate of new bone formation by micro-CT was lower than previous studies perhaps due to the utilization of different cell types (hPDLs vs. ADSCs), different scaffold (PCL vs. apatite-coated) and different in immunologic reaction of mice model (C57BL mice vs. nude mice) [97-99].

Next, the immunohistochemical analysis specific to human cells was performed to evaluate the existence and role of hPDLs in the graft. The samples with defect or scaffold only did not show the positive staining of human Integrin β_1. Only the samples grafted with hPDLs showed the positive staining. Integrins are α/β heterodimeric cell surface receptors that play a pivotal role in cell adhesion and migration, as well as in growth and survival. The β_1 subfamily includes 12 distinct integrin proteins that bind to different extracellular matrix molecules [100]. Control of extracellular integrin binding influences cell adhesion and migration, while intracellular signaling messages relayed by the β_1 cytoplasmic tail help to regulate cell proliferation, cytoskeletal reorganization, and gene expression. Previous studies showed that β_1 expressed in hPDLs and was up-regulated markedly during mechano-transduction in bone cells. It has been reported that bioadhesive material stimulates osteogenic differentiation of PDL stem cells via activation of the integrin β_1 [101, 102]. The results indicated that hPDLs can survive and repopulate in the defect. Previous study was also successful in detecting human MSCs and osteoblast-like cells in rat calvarium [96]. In fact, xenogenic transplantation may have a practical significance in future clinical applications, especially in the bone regenerating for aged patients. New bone formation can be from host bone cells/ periostem cells and/or

implanted cells. Xenograft of hMSCs can induce bone-related genes in animal host cells. For instant, gene activation in bone defect of rat after hMSC transplantation included osteogenesis-related markers, osteo-trophic factors (*ALP, OPN, VEGF, IGF-1, BMP-2, SDF-1* and *OPG*), as well as ECM-related genes (*COL1* and *FN*) [103]. The disappearance of hMSCs from the implantation site after 2 weeks indicated that hMSC were inducers rather than effectors of bone formation [104]. Additionally, studies showed that HDAC inhibitors (VPA, TSA) can induce trophic factor mRNA such as *BMP-2, BMP-4* in hMSCs, ADSCs, primary dental pulp cells [48, 84, 105]. More investigations are needed to verify HDAC inhibitor can induce hPDLs to drive mouse cells into osteogenic differentiation via paracrine mode.

The immunogenicity of foreign cells in the recipient is an important problem in clinical cell transplantation. Previous studies demonstrated that both undifferentiated and differentiated MSCs have low immunogenic profiles which do not elicit local or systemic rejection reactions after transplantation [106-109]. Our result showed that total mouse serum IgG increased significantly in all surgical groups comparing with baseline at 4 weeks after surgery. However, there was no significant difference between groups in both time points. This phenomenon might indicate that increase in total serum IgG in experiment groups is likely a result of operative procedure rather than foreign materials induction. During the convenient setup of operation, inflammation and infection can affect the immune status of animals. IgG, which is produced by B plasma cells, is a major component of humoral immunity which is the most common type of antibody found in the circulation (75%). IgG bind to antigens on cell surface or extracellular matrix, neutralize and target them for phagocytosis and also activate the complement system with high affinity [110, 111].

We further investigated whether or not hPDLs induce immune response in mouse by examining hPDLs-specific mouse IgG by ELISA. The empty ELISA wells were covered by hPDLs lysate to capture anti-human mouse IgG in the serum. The positive control was generated by injection of hPDL lysate with adjuvant into the mice. Antigens from hPDLs are foreign proteins (associate with strong adjuvants) that enter the mouse body. They are first concentrated in the lymph nodes, spleen, and other lymphoid tissues leading to activation of helper T-cells. These helper T cells secrete cytokines that interact with the antigen-specific B cells and enhance antibody secretion; ie. IgG. In fact, helper T cells are absolutely required for effective IgG responses against protein antigens. This process calls T cell dependent antibody response [110, 111]. In general, our method is the most convenient way to verify the response of animal body with human antigen via the activation of T helper cells and B cells. The serum from mice immunized with hPDLs lysate demonstrated the significant increase in hPDLs-specific IgG. Although there were a slight different in hPDLs-specific IgG in groups with hPDLs (with and without TSA) comparing with negative control groups (defect and scaffold only), the levels were not significant. In fact, it exhibited an immunological response against human cell in mice model but this response is not strong enough to affect total IgG levels. In PDL stem cells and stromal cells, several studies showed that these cells have an immunomodulatory ability that is comparable to bone marrow MSCs [112]. They possessed low immunogenicity due to the absence of HLA- II DR or T cell co-stimulatory molecules [113, 114]. Moreover, these cells inhibited proliferation of allogeneic T cells through upregulation of cyclooxygenase-2 and prostaglandin E2. The inhibitory effect on T cell proliferation was intact after osteogenic induction [115]. Additionally, PDL stem

cells also suppressed B cells proliferation, differentiation and migration through cell-to-cell contact [116]. The low immunogenicity and immunosuppressive effects allow use of PDLs in periodontal regeneration. For example, allogeneic PDL stem cells have been tested in a sheep and a swine model showing the equal therapeutic effects to those of autologous grafts [116-118]. In general, the foreign body reaction composed of macrophages and foreign body giant cells is the end-stage response of the inflammatory and wound healing responses following implantation of a medical device, prosthesis, or biomaterial [119]. Though the total and hPDLs-specific mouse IgG might not enough to prove the presentation of a local immunological response and inflammation, it can partly show that there was little, not significant, immunological response of mice against hPDLs in our *in vivo* model, therefor confirming the successfulness of our method.

Up to date, HDAC inhibitors are used in studies to cure nerve degradation, inflammation and cancer [32, 37-39]. The inhibitors are also considered in bone related therapies such as tissue engineering for bone regeneration. Our results demonstrated that TSA enhances osteogenic differentiation of hPDLs *in vitro* suggesting that regulation of histone acetylation may be useful for promoting bone formation (Fig 5.1). However, more studies are needed to elucidate the precise functions of HDACs and possible side effects of the inhibitor with long term administration should be approached with carefulness.
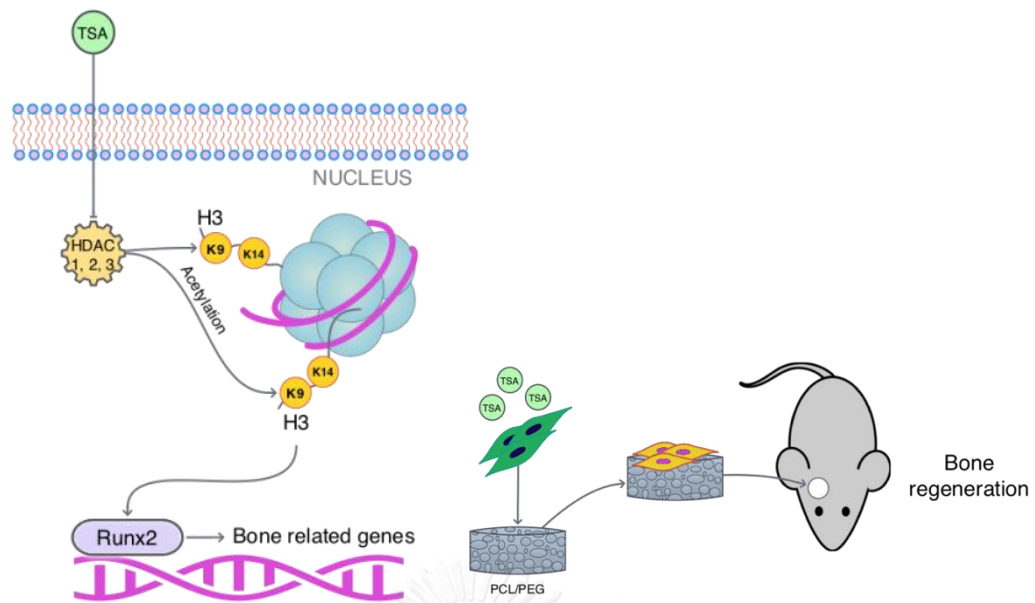
Figure 5.1: Suggestion mechanism of TSA in osteogenic differentiation of hPDLs (left) and application in bone regeneration (right). TSA inhibits HDAC enzymes, including the reduction of HDAC1, 2, 3 leading to the acetylation of H3K9K14 and production of RUNX2 which activate bone related gene expression. Then, the cells go to osteogenesis. The combination of TSA, cells and scaffold can be applied in bone regeneration. H3: Histone H3; K9, K14: Lysine 9, 14.

In conclusion, hPDLs express a series of HDAC enzymes with are distinctive from other cell types. Inhibition of the activity of class I and II HDACs promoted osteogenic differentiation; probably partly via HDAC 3 leading to the acetylation of H3K9K14 and RUNX2. TSA enhance new bone formation in mouse calvarial defect model by PCL/PEG scaffold and hPDLs. This finding suggests a potential application of TSA for bone regeneration therapy by hPDLs.

REFERENCES

1.   Avery JK, Chiego DJ. Essentials of oral histology and embryology: a clinical approach. Missouri: Mosby Elsevier; 2006.

2.   Bergomi M, Cugnoni J, Galli M, Botsis J, Belser UC, Wiskott HW. Hydro-mechanical coupling in the periodontal ligament: a porohyperelastic finite element model. Journal of biomechanics. 2011;44(1):34-8.

3.   Seo BM, Miura M, Gronthos S, Bartold PM, Batouli S, Brahim J, et al. Investigation of multipotent postnatal stem cells from human periodontal ligament. Lancet. 2004;364(9429):149-55.

4.   Gay IC, Chen S, MacDougall M. Isolation and characterization of multipotent human periodontal ligament stem cells. Orthodontics & craniofacial research. 2007;10(3):149-60.

5.   Kaneda T, Miyauchi M, Takekoshi T, Kitagawa S, Kitagawa M, Shiba H, et al. Characteristics of periodontal ligament subpopulations obtained by sequential enzymatic digestion of rat molar periodontal ligament. Bone. 2006;38(3):420-6.

6.   Zhou Y, Fu Y, Li JP, Qi LY. The role of estrogen in osteogenetic cytokine expression in human periodontal ligament cells. The International journal of periodontics & restorative dentistry. 2009;29(5):507-13.

7.   Choi HD, Noh WC, Park JW, Lee JM, Suh JY. Analysis of gene expression during mineralization of cultured human periodontal ligament cells. Journal of periodontal & implant science. 2011;41(1):30-43.

8.   Cho HH, Park HT, Kim YJ, Bae YC, Suh KT, Jung JS. Induction of osteogenic differentiation of human mesenchymal stem cells by histone deacetylase inhibitors. Journal of cellular biochemistry. 2005;96(3):533-42.

9.   Schroeder TM, Westendorf JJ. Histone deacetylase inhibitors promote osteoblast maturation. Journal of bone and mineral research : the official journal of the American Society for Bone and Mineral Research. 2005;20(12):2254-63.

10.   Xu Y, Hammerick KE, James AW, Carre AL, Leucht P, Giaccia AJ, et al. Inhibition of histone deacetylase activity in reduced oxygen environment enhances the osteogenesis of mouse adipose-derived stromal cells. Tissue engineering Part A. 2009;15(12):3697-707.

11.   Buchwald M, Kramer OH, Heinzel T. HDACi--targets beyond chromatin. Cancer letters. 2009;280(2):160-7.

12.   de Ruijter AJ, van Gennip AH, Caron HN, Kemp S, van Kuilenburg AB. Histone deacetylases (HDACs): characterization of the classical HDAC family. The Biochemical journal. 2003;370(Pt 3):737-49.

13.   Dokmanovic M, Clarke C, Marks PA. Histone deacetylase inhibitors: overview and perspectives. Molecular cancer research : MCR. 2007;5(10):981-9.

14.   Zhao X, Ruan Y, Wei CL. Tackling the epigenome in the pluripotent stem cells. Journal of genetics and genomics = Yi chuan xue bao. 2008;35(7):403-12.

15.   Alberts B. DNA and Chromosomes. Essential Cell Biology. 3rd ed: Garland Science; 2010. p. 171-95.

16.   Gregory PD, Wagner K, Horz W. Histone acetylation and chromatin remodeling. Experimental cell research. 2001;265(2):195-202.

17.   Barrero MJ, Boue S, Izpisua Belmonte JC. Epigenetic mechanisms that regulate cell identity. Cell stem cell. 2010;7(5):565-70.

18.   Gordon JA, Montecino MA, Aqeilan RI, Stein JL, Stein GS, Lian JB. Epigenetic pathways regulating bone homeostasis: potential targeting for intervention of skeletal disorders. Current osteoporosis reports. 2014;12(4):496-506.

19.   Bjerling P, Silverstein RA, Thon G, Caudy A, Grewal S, Ekwall K. Functional divergence between histone deacetylases in fission yeast by distinct cellular localization and in vivo specificity. Molecular and cellular biology. 2002;22(7):2170-81.

20.   Yan C, Boyd DD. Histone H3 acetylation and H3 K4 methylation define distinct chromatin regions permissive for transgene expression. Molecular and cellular biology. 2006;26(17):6357-71.

21.   Shukla V, Vaissiere T, Herceg Z. Histone acetylation and chromatin signature in stem cell identity and cancer. Mutation research. 2008;637(1-2):1-15.

22.   Zeng L, Zhou MM. Bromodomain: an acetyl-lysine binding domain. FEBS Lett. 2002;513(1):124-8.

23.   Jenuwein T, Allis CD. Translating the histone code. Science. 2001;293(5532):1074-80.

24.   Roth SY, Denu JM, Allis CD. Histone acetyltransferases. Annual review of biochemistry. 2001;70:81-120.

25.   Gregoretti IV, Lee YM, Goodson HV. Molecular evolution of the histone deacetylase family: functional implications of phylogenetic analysis. Journal of molecular biology. 2004;338(1):17-31.

26.   Choudhary C, Kumar C, Gnad F, Nielsen ML, Rehman M, Walther TC, et al. Lysine acetylation targets protein complexes and co-regulates major cellular functions. Science. 2009;325(5942):834-40.

27.   Haberland M, Montgomery RL, Olson EN. The many roles of histone deacetylases in development and physiology: implications for disease and therapy. Nature reviews Genetics. 2009;10(1):32-42.

28.   Seto E. The biology of HDAC3. In: Verdin E, editor. Histone Deacetylases. New Jersey: Springer; 2006. p. 61-86.

29.   Palmieri C, Coombes RC, Vigushin DM. Targeted histone deacetylase inhibition for cancer prevention and therapy. Progress in drug research Fortschritte der Arzneimittelforschung Progres des recherches pharmaceutiques. 2005;63:147-81.

30.   Marks PA. Histone deacetylase inhibitors: a chemical genetics approach to understanding cellular functions. Biochimica et biophysica acta. 2010;1799(10-12):717-25.

31.   Vega RB, Matsuda K, Oh J, Barbosa AC, Yang X, Meadows E, et al. Histone deacetylase 4 controls chondrocyte hypertrophy during skeletogenesis. Cell. 2004;119(4):555-66.

32.   Witt O, Deubzer HE, Milde T, Oehme I. HDAC family: What are the cancer relevant targets? Cancer letters. 2009;277(1):8-21.

33.   Tong JJ, Liu J, Bertos NR, Yang XJ. Identification of HDAC10, a novel class II human histone deacetylase containing a leucine-rich domain. Nucleic acids research. 2002;30(5):1114-23.

34.   Villagra A, Cheng F, Wang HW, Suarez I, Glozak M, Maurin M, et al. The histone deacetylase HDAC11 regulates the expression of interleukin 10 and immune tolerance. Nature immunology. 2009;10(1):92-100.

35.   Suzuki T. Explorative study on isoform-selective histone deacetylase inhibitors. Chemical & pharmaceutical bulletin. 2009;57(9):897-906.

36.   Zhang B, West EJ, Van KC, Gurkoff GG, Zhou J, Zhang XM, et al. HDAC inhibitor increases histone H3 acetylation and reduces microglia inflammatory response following traumatic brain injury in rats. Brain research. 2008;1226:181-91.

37.   Dash PK, Orsi SA, Moore AN. Histone deactylase inhibition combined with behavioral therapy enhances learning and memory following traumatic brain injury. Neuroscience. 2009;163(1):1-8.

38.   Toussirot E, Khan KA, Bertolini E, Wendling D, Herbein G. Histone deacetylase inhibitors: new treatment options for inflammatory joint disease? Joint, bone, spine : revue du rhumatisme. 2010;77(5):395-8.

39.   Lu J, Yang C, Chen M, Ye DY, Lonser RR, Brady RO, et al. Histone deacetylase inhibitors prevent the degradation and restore the activity of glucocerebrosidase in Gaucher disease. Proceedings of the National Academy of Sciences of the United States of America. 2011;108(52):21200-5.

40.   Aubin JE. Mesenchymal Stem Cells and Osteoblast Differentiation. In: Bilezikian JP, Raisz LG, Martin TJ, editors. Principles of Bone Biology, Two-Volume Set. 1. 3rd ed: Elsevier Science; 2008. p. 85-107.

41.   Eroschenko VP. Bone. DiFiore's Atlas of Histology With Functional Correlations. 11th ed: Wolters Kluwer Health/Lippincott Williams & Wilkins; 2008. p. 79-98.

42.   Datta HK, Ng WF, Walker JA, Tuck SP, Varanasi SS. The cell biology of bone metabolism. Journal of clinical pathology. 2008;61(5):577-87.

43.   Schinke T, Karsenty G. Transcriptional Control of Osteoblast Differentiation and Function. In: Bilezikian JP, Raisz LG, Martin TJ, editors. Principles of Bone Biology, Two-Volume Set. 1. 3rd ed: Elsevier Science; 2008. p. 109-19.

44.   Liu F, Malaval L, Aubin JE. Global amplification polymerase chain reaction reveals novel transitional stages during osteoprogenitor differentiation. Journal of cell science. 2003;116(Pt 9):1787-96.

45.   Shen J, Montecino M, Lian JB, Stein GS, Van Wijnen AJ, Stein JL. Histone acetylation in vivo at the osteocalcin locus is functionally linked to vitamin D-dependent, bone tissue-specific transcription. The Journal of biological chemistry. 2002;277(23):20284-92.

46.   Shen J, Hovhannisyan H, Lian JB, Montecino MA, Stein GS, Stein JL, et al. Transcriptional induction of the osteocalcin gene during osteoblast differentiation involves acetylation of histones h3 and h4. Mol Endocrinol. 2003;17(4):743-56.

47.   Westendorf JJ, Zaidi SK, Cascino JE, Kahler R, van Wijnen AJ, Lian JB, et al. Runx2 (Cbfa1, AML-3) interacts with histone deacetylase 6 and represses the p21(CIP1/WAF1) promoter. Molecular and cellular biology. 2002;22(22):7982-92.

48.   Xu S, De Veirman K, Evans H, Santini GC, Vande Broek I, Leleu X, et al. Effect of the HDAC inhibitor vorinostat on the osteogenic differentiation of mesenchymal stem cells in vitro and bone formation in vivo. Acta pharmacologica Sinica. 2013;34(5):699-709.

49.   Schroeder TM, Kahler RA, Li X, Westendorf JJ. Histone deacetylase 3 interacts with runx2 to repress the osteocalcin promoter and regulate osteoblast differentiation. The Journal of biological chemistry. 2004;279(40):41998-2007.

50.   Lee HW, Suh JH, Kim AY, Lee YS, Park SY, Kim JB. Histone deacetylase 1-mediated histone modification regulates osteoblast differentiation. Mol Endocrinol. 2006;20(10):2432-43.

51.   Fu Y, Zhang P, Ge J, Cheng J, Dong W, Yuan H, et al. Histone deacetylase 8 suppresses osteogenic differentiation of bone marrow stromal cells by inhibiting histone H3K9 acetylation and RUNX2 activity. The international journal of biochemistry & cell biology. 2014;54:68-77.

52.   Paino F, La Noce M, Tirino V, Naddeo P, Desiderio V, Pirozzi G, et al. Histone deacetylase inhibition with valproic acid downregulates osteocalcin gene expression in human dental pulp stem cells and osteoblasts: evidence for HDAC2 involvement. Stem Cells. 2014;32(1):279-89.

53.   Cao K, Wei L, Zhang Z, Guo L, Zhang C, Li Y, et al. Decreased histone deacetylase 4 is associated with human osteoarthritis cartilage degeneration by releasing histone deacetylase 4 inhibition of runt-related transcription factor-2 and increasing osteoarthritis-related genes: a novel mechanism of human osteoarthritis cartilage degeneration. Arthritis research & therapy. 2014;16(6):491.

54.   Lu J, Sun Y, Ge Q, Teng H, Jiang Q. Histone deacetylase 4 alters cartilage homeostasis in human osteoarthritis. BMC musculoskeletal disorders. 2014;15:438.

55.   Kim K, Lee J, Kim JH, Jin HM, Zhou B, Lee SY, et al. Protein inhibitor of activated STAT 3 modulates osteoclastogenesis by down-regulation of NFATc1 and osteoclast-associated receptor. J Immunol. 2007;178(9):5588-94.

56.   Destaing O, Saltel F, Gilquin B, Chabadel A, Khochbin S, Ory S, et al. A novel Rho-mDia2-HDAC6 pathway controls podosome patterning through microtubule acetylation in osteoclasts. Journal of cell science. 2005;118(Pt 13):2901-11.

57.   Pham L, Kaiser B, Romsa A, Schwarz T, Gopalakrishnan R, Jensen ED, et al. HDAC3 and HDAC7 have opposite effects on osteoclast differentiation. The Journal of biological chemistry. 2011;286(14):12056-65.

58.   Jin Z, Wei W, Dechow PC, Wan Y. HDAC7 inhibits osteoclastogenesis by reversing RANKL-triggered beta-catenin switch. Mol Endocrinol. 2013;27(2):325-35.

59.   Westendorf JJ. Histone deacetylases in control of skeletogenesis. Journal of cellular biochemistry. 2007;102(2):332-40.

60.   McGee-Lawrence ME, Westendorf JJ. Histone deacetylases in skeletal development and bone mass maintenance. Gene. 2011;474(1-2):1-11.

61.   Polo-Corrales L, Latorre-Esteves M, Ramirez-Vick JE. Scaffold design for bone regeneration. J Nanosci Nanotechnol. 2014;14(1):15-56.

62.   Thadavirul N, Pavasant P, Supaphol P. Improvement of dual-leached polycaprolactone porous scaffolds by incorporating with hydroxyapatite for bone tissue regeneration. Journal of biomaterials science Polymer edition. 2014;25(17):1986-2008.

63.   Rezwan K, Chen QZ, Blaker JJ, Boccaccini AR. Biodegradable and bioactive porous polymer/inorganic composite scaffolds for bone tissue engineering. Biomaterials. 2006;27(18):3413-31.

64.   Thadavirul N, Pavasant P, Supaphol P. Development of polycaprolactone porous scaffolds by combining solvent casting, particulate leaching, and polymer leaching techniques for bone tissue engineering. Journal of biomedical materials research Part A. 2014;102(10):3379-92.

65. Gomes PS, Fernandes MH. Rodent models in bone-related research: the relevance of calvarial defects in the assessment of bone regeneration strategies. Laboratory animals. 2011;45(1):14-24.

66. Gupta DM, Kwan MD, Slater BJ, Wan DC, Longaker MT. Applications of an athymic nude mouse model of nonhealing critical-sized calvarial defects. The Journal of craniofacial surgery. 2008;19(1):192-7.

67. Seo BM, Sonoyama W, Yamaza T, Coppe C, Kikuiri T, Akiyama K, et al. SHED repair critical-size calvarial defects in mice. Oral diseases. 2008;14(5):428-34.

68. Cooper GM, Mooney MP, Gosain AK, Campbell PG, Losee JE, Huard J. Testing the critical size in calvarial bone defects: revisiting the concept of a critical-size defect. Plastic and reconstructive surgery. 2010;125(6):1685-92.

69. Osathanon T, Vivatbutsiri P, Sukarawan W, Sriarj W, Pavasant P, Sooampon S. Cobalt chloride supplementation induces stem-cell marker expression and inhibits osteoblastic differentiation in human periodontal ligament cells. Archives of oral biology. 2015;60(1):29-36.

70. Yoshida M, Kijima M, Akita M, Beppu T. Potent and specific inhibition of mammalian histone deacetylase both in vivo and in vitro by trichostatin A. The Journal of biological chemistry. 1990;265(28):17174-9.

71. Chuenjitkuntaworn B, Inrung W, Damrongsri D, Mekaapiruk K, Supaphol P, Pavasant P. Polycaprolactone/hydroxyapatite composite scaffolds: preparation, characterization, and in vitro and in vivo biological responses of human primary bone cells. Journal of biomedical materials research Part A. 2010;94(1):241-51.

72. Osathanon T, Ritprajak P, Nowwarote N, Manokawinchoke J, Giachelli C, Pavasant P. Surface-bound orientated Jagged-1 enhances osteogenic differentiation of

human periodontal ligament-derived mesenchymal stem cells. Journal of biomedical materials research Part A. 2013;101(2):358-67.

73.   Jensen ED, Schroeder TM, Bailey J, Gopalakrishnan R, Westendorf JJ. Histone deacetylase 7 associates with Runx2 and represses its activity during osteoblast maturation in a deacetylation-independent manner. Journal of bone and mineral research : the official journal of the American Society for Bone and Mineral Research. 2008;23(3):361-72.

74.   Choo MK, Yeo H, Zayzafoon M. NFATc1 mediates HDAC-dependent transcriptional repression of osteocalcin expression during osteoblast differentiation. Bone. 2009;45(3):579-89.

75.   Kim TI, Han JE, Jung HM, Oh JH, Woo KM. Analysis of histone deacetylase inhibitor-induced responses in human periodontal ligament fibroblasts. Biotechnol Lett. 2013;35(1):129-33.

76.   Gregoire S, Xiao L, Nie J, Zhang X, Xu M, Li J, et al. Histone deacetylase 3 interacts with and deacetylates myocyte enhancer factor 2. Molecular and cellular biology. 2007;27(4):1280-95.

77.   Leupin O, Kramer I, Collette NM, Loots GG, Natt F, Kneissel M, et al. Control of the SOST bone enhancer by PTH using MEF2 transcription factors. Journal of bone and mineral research : the official journal of the American Society for Bone and Mineral Research. 2007;22(12):1957-67.

78.   Baertschi S, Baur N, Lueders-Lefevre V, Voshol J, Keller H. Class I and IIa histone deacetylases have opposite effects on sclerostin gene regulation. The Journal of biological chemistry. 2014;289(36):24995-5009.

79.   Golub EE, Boesze-Battaglia K. The role of alkaline phosphatase in mineralization. Current Opinion in Orthopaedics. 2007;18(5):444-8.

80.   Id Boufker H, Lagneaux L, Najar M, Piccart M, Ghanem G, Body JJ, et al. The Src inhibitor dasatinib accelerates the differentiation of human bone marrow-derived mesenchymal stromal cells into osteoblasts. BMC cancer. 2010;10:298.

81.   Tanaka K, Iwasaki K, Feghali KE, Komaki M, Ishikawa I, Izumi Y. Comparison of characteristics of periodontal ligament cells obtained from outgrowth and enzyme-digested culture methods. Archives of oral biology. 2011;56(4):380-8.

82.   Zhou Y, Hutmacher DW, Sae-Lim V, Zhou Z, Woodruff M, Lim TM. Osteogenic and adipogenic induction potential of human periodontal cells. Journal of periodontology. 2008;79(3):525-34.

83.   Haberland M, Carrer M, Mokalled MH, Montgomery RL, Olson EN. Redundant control of adipogenesis by histone deacetylases 1 and 2. The Journal of biological chemistry. 2010;285(19):14663-70.

84.   Hu X, Zhang X, Dai L, Zhu J, Jia Z, Wang W, et al. Histone deacetylase inhibitor trichostatin A promotes the osteogenic differentiation of rat adipose-derived stem cells by altering the epigenetic modifications on Runx2 promoter in a BMP signaling-dependent manner. Stem cells and development. 2013;22(2):248-55.

85.   Qiao Y, Wang R, Yang X, Tang K, Jing N. Dual roles of histone h3 lysine 9 acetylation in human embryonic stem cell pluripotency and neural differentiation. The Journal of biological chemistry. 2015;290(4):2508-20.

86.   Silverstein RA, Ekwall K. Sin3: a flexible regulator of global gene expression and genome stability. Curr Genet. 2005;47(1):1-17.

87.   Westendorf JJ. Transcriptional co-repressors of Runx2. Journal of cellular biochemistry. 2006;98(1):54-64.

88.   Hesse E, Saito H, Kiviranta R, Correa D, Yamana K, Neff L, et al. Zfp521 controls bone mass by HDAC3-dependent attenuation of Runx2 activity. The Journal of cell biology. 2010;191(7):1271-83.

89.   Jeon EJ, Lee KY, Choi NS, Lee MH, Kim HN, Jin YH, et al. Bone morphogenetic protein-2 stimulates Runx2 acetylation. The Journal of biological chemistry. 2006;281(24):16502-11.

90.   Jonason JH, Xiao G, Zhang M, Xing L, Chen D. Post-translational Regulation of Runx2 in Bone and Cartilage. Journal of dental research. 2009;88(8):693-703.

91.   Bae SC, Lee YH. Phosphorylation, acetylation and ubiquitination: the molecular basis of RUNX regulation. Gene. 2006;366(1):58-66.

92.   Xu Y, Voelter-Mahlknecht S, Mahlknecht U. The histone deacetylase inhibitor suberoylanilide hydroxamic acid down-regulates expression levels of Bcr-abl, c-Myc and HDAC3 in chronic myeloid leukemia cell lines. International journal of molecular medicine. 2005;15(1):169-72.

93.   Hoque ME, San WY, Wei F, Li S, Huang MH, Vert M, et al. Processing of polycaprolactone and polycaprolactone-based copolymers into 3D scaffolds, and their cellular responses. Tissue engineering Part A. 2009;15(10):3013-24.

94.   Chuenjitkuntaworn B, Osathanon T, Nowwarote N, Supaphol P, Pavasant P. The efficacy of polycaprolactone/hydroxyapatite scaffold in combination with mesenchymal stem cells for bone tissue engineering. Journal of biomedical materials research Part A. 2016;104(1):264-71.

95. Jin H, Park JY, Choi H, Choung PH. HDAC inhibitor trichostatin A promotes proliferation and odontoblast differentiation of human dental pulp stem cells. Tissue engineering Part A. 2013;19(5-6):613-24.

96. Zong C, Xue D, Yuan W, Wang W, Shen D, Tong X, et al. Reconstruction of rat calvarial defects with human mesenchymal stem cells and osteoblast-like cells in poly-lactic-co-glycolic acid scaffolds. European cells & materials. 2010;20:109-20.

97. Levi B, Nelson ER, Li S, James AW, Hyun JS, Montoro DT, et al. Dura mater stimulates human adipose-derived stromal cells to undergo bone formation in mouse calvarial defects. Stem Cells. 2011;29(8):1241-55.

98. Levi B, James AW, Nelson ER, Peng M, Wan DC, Commons GW, et al. Acute skeletal injury is necessary for human adipose-derived stromal cell-mediated calvarial regeneration. Plastic and reconstructive surgery. 2011;127(3):1118-29.

99. Levi B, James AW, Nelson ER, Vistnes D, Wu B, Lee M, et al. Human adipose derived stromal cells heal critical size mouse calvarial defects. PloS one. 2010;5(6):e11177.

100. Liu S, Calderwood DA, Ginsberg MH. Integrin cytoplasmic domain-binding proteins. Journal of cell science. 2000;113 (Pt 20):3563-71.

101. Lee JS, Yi JK, An SY, Heo JS. Increased osteogenic differentiation of periodontal ligament stem cells on polydopamine film occurs via activation of integrin and PI3K signaling pathways. Cellular physiology and biochemistry : international journal of experimental cellular physiology, biochemistry, and pharmacology. 2014;34(5):1824-34.

102. Ziegler N, Alonso A, Steinberg T, Woodnutt D, Kohl A, Müssig E, et al. Mechano-transduction in periodontal ligament cells identifies activated states of

MAP-kinases p42/44 and p38-stress kinase as a mechanism for MMP-13 expression. BMC Cell Biology. 2010;11(1):1-14.

103. Hwang SJ, Cho TH, Kim IS. In vivo gene activity of human mesenchymal stem cells after scaffold-mediated local transplantation. Tissue engineering Part A. 2014;20(17-18):2350-64.

104. Gamblin AL, Brennan MA, Renaud A, Yagita H, Lezot F, Heymann D, et al. Bone tissue formation with human mesenchymal stem cells and biphasic calcium phosphate ceramics: the local implication of osteoclasts and macrophages. Biomaterials. 2014;35(36):9660-7.

105. Duncan HF, Smith AJ, Fleming GJ, Cooper PR. Histone deacetylase inhibitors epigenetically promote reparative events in primary dental pulp cells. Experimental cell research. 2013;319(10):1534-43.

106. Le Blanc K, Tammik C, Rosendahl K, Zetterberg E, Ringden O. HLA expression and immunologic properties of differentiated and undifferentiated mesenchymal stem cells. Exp Hematol. 2003;31(10):890-6.

107. Pierdomenico L, Bonsi L, Calvitti M, Rondelli D, Arpinati M, Chirumbolo G, et al. Multipotent mesenchymal stem cells with immunosuppressive activity can be easily isolated from dental pulp. Transplantation. 2005;80(6):836-42.

108. Niemeyer P, Schonberger TS, Hahn J, Kasten P, Fellenberg J, Suedkamp N, et al. Xenogenic transplantation of human mesenchymal stem cells in a critical size defect of the sheep tibia for bone regeneration. Tissue engineering Part A. 2010;16(1):33-43.

109. Niemeyer P, Kornacker M, Mehlhorn A, Seckinger A, Vohrer J, Schmal H, et al. Comparison of immunological properties of bone marrow stromal cells and

adipose tissue-derived stem cells before and after osteogenic differentiation in vitro. Tissue engineering. 2007;13(1):111-21.

110.   Abbas AK, Lichtman AHH, Pillai S. Basic Immunology: Functions and Disorders of the Immune System. 4th ed: Elsevier Health Sciences; 2012.

111.   Alberts B. Molecular Biology of the Cell: Reference edition: Garland Science; 2008.

112.   Zhu W, Liang M. Periodontal ligament stem cells: current status, concerns, and future prospects. Stem cells international. 2015;2015:972313.

113.   Wada N, Menicanin D, Shi S, Bartold PM, Gronthos S. Immunomodulatory properties of human periodontal ligament stem cells. Journal of cellular physiology. 2009;219(3):667-76.

114.   Vasandan AB, Shankar SR, Prasad P, Sowmya Jahnavi V, Bhonde RR, Jyothi Prasanna S. Functional differences in mesenchymal stromal cells from human dental pulp and periodontal ligament. J Cell Mol Med. 2014;18(2):344-54.

115.   Tang R, Wei F, Wei L, Wang S, Ding G. Osteogenic differentiated periodontal ligament stem cells maintain their immunomodulatory capacity. Journal of tissue engineering and regenerative medicine. 2014;8(3):226-32.

116.   Liu O, Xu J, Ding G, Liu D, Fan Z, Zhang C, et al. Periodontal ligament stem cells regulate B lymphocyte function via programmed cell death protein 1. Stem Cells. 2013;31(7):1371-82.

117.   Mrozik KM, Wada N, Marino V, Richter W, Shi S, Wheeler DL, et al. Regeneration of periodontal tissues using allogeneic periodontal ligament stem cells in an ovine model. Regenerative medicine. 2013;8(6):711-23.

118. Ding G, Liu Y, Wang W, Wei F, Liu D, Fan Z, et al. Allogeneic periodontal ligament stem cell therapy for periodontitis in swine. Stem Cells. 2010;28(10):1829-38.

119. Trindade R, Albrektsson T, Tengvall P, Wennerberg A. Foreign Body Reaction to Biomaterials: On Mechanisms for Buildup and Breakdown of Osseointegration. Clin Implant Dent Relat Res. 2016;18(1):192-203.

VITA

Mr. Huynh Cong Nhat Nam was born in Nha Trang city, a beautiful seaside city in the middle of Vietnam. He graduated DDS from the Medicine and Pharmacy University, Ho Chi Minh city. At the moment, he is participating in PhD program in Oral Biology at Chulalongkorn University, Bangkok. He is a motivating and dynamic youth with big ambitions.

Awards and Honors:

2004: Graduate from high school with coming first in this exam in Khanh Hoa province. Pass the Medicine and Pharmacy University entrance exam with the runner up.

2010: Get the best result for the undergraduate thesis for doctor of dental surgery.

2011: First prize of Vietnam Dental student travel award in scientific study.

2012: First prize of The 22nd Conference of science and technology for the youth of University of Medicine and Pharmacy- Ho Chi Minh city. First prize of The 16nd Conference of science and technology for the youth of National Medicine and Pharmacy Universities, Nam Dinh city, Vietnam.

2015: Young investigator award of 13th Congress of international society of bone morphometry, TMDU - Tokyo, May 27-29th.

2015: Winner of Postgraduate Poster Presentation Competion of The 13th National Scientific Conference of The Dental Faculty Consortiun of Thailand- DFCT 2015, Chulalongkorn University, Bangkok, July 22-24th.

Research Fields: Basic oral microbiology, dental stem cells and bone biology study.

Publications:

Huynh Cong Nhat Nam, Ngo Thi Quynh Lan, Dang Vu Ngoc Mai. (2011) The efficiency of milk and egg white in storage of avulsed teeth, Medical Journal of Ho Chi Minh city, 15(2): 82-89.

Vo Manh Hung, Dang Vu Ngoc Mai, Huynh Cong Nhat Nam. (2014) The effect of probiotic-containing yogurt on the number of volatile sulfur compounds producing bacteria on the dorsal surface of tongue. Medical Journal of Ho Chi Minh city, 18(1): 347-351.

Huynh NC, Everts V, Pavasant P, Ampornaramveth RS. (2016) Inhibition of Histone Deacetylases Enhances the Osteogenic Differentiation of Human Periodontal Ligament Cells. Journal of cellular biochemistry, 117:1384-1395.